

Kinematics of the Middle East and Eastern Mediterranean Updated

ROB WESTAWAY

16 Neville Square, Durham DH1 3PY, ENGLAND
(e-mail: r.w.c.westaway@ncl.ac.uk)

Abstract: A revised quantitative, internally consistent, kinematic model has been determined for the present-day relative plate motions in the eastern Mediterranean and Middle Eastern regions, based on a combination of geological and GPS data. The relative motions of the brittle upper crust of the African and Arabian plates across the southern Dead Sea Fault Zone (DSFZ) are represented by relative rotation at $0.278^\circ \text{Ma}^{-1}$ about an Euler pole at $31.1^\circ\text{N } 26.7^\circ\text{E}$. The resulting predicted slip rate on the southern DSFZ is 4.0 mm a^{-1} . The kinematics of the northern DSFZ are described as relative rotation at $0.243^\circ \text{Ma}^{-1}$ about the same Euler pole, the difference in rotation rates reflecting the absorption of a small component of the relative motion by distributed shortening in the Palmyra fold belt. The northern DSFZ, in Syria and southern Turkey, is regarded as a series of transpressional stepovers, along which the rate of left-lateral slip is substantially less than the rate of relative plate motion, because this slip is oriented strongly obliquely to the relative motion between the adjoining plates. This geometry seems to result in part from some strands of the northern DSFZ reactivating older fault segments, even though they were not optimally oriented relative to the plate motion, and in part because the ideal initial geometry of the DSFZ, which would have continued northwestward offshore of the Levant coastline towards Cyprus, was precluded by the high strength of the crust along this line. The revised slip rate on the East Anatolian Fault Zone (EAFZ) is estimated as $\sim 8 \text{ mm a}^{-1}$. At this rate, restoring the observed slip requires the age of the EAFZ to be $\sim 4 \text{ Ma}$. The previous phase of deformation, which involved slip on the Malatya-Ovacik Fault Zone before the EAFZ came into being, is thus dated to $\sim 7\text{--}4 \text{ Ma}$, suggesting a timing of initiation for the North Anatolian Fault Zone (NAFZ) of $\sim 7 \text{ Ma}$, not $\sim 5 \text{ Ma}$ as has previously been thought. Local evidence from the western NAFZ also supports a $\sim 7 \text{ Ma}$ or Early Messinian age for the NAFZ. The overall present-day kinematics of the NAFZ are described using the Euler vector determined in 2000 using GPS: involving relative rotation between the Turkish and Eurasian plates at 1.2°Ma^{-1} about $30.7^\circ\text{N } 32.6^\circ\text{E}$. This Euler vector predicts a rate of relative motion between these plates of $\sim 25 \text{ mm a}^{-1}$, which when extrapolated overestimates the observed amount of localised right-lateral slip, suggesting the existence of a component of distributed right-lateral simple shear in the surroundings to the NAFZ as well. The predicted rate of left-lateral relative motion on the boundary between the Turkish and African plates is estimated as $\sim 8 \text{ mm a}^{-1}$. However, the rate of localised left-lateral slip on the onshore part of this boundary is estimated as only $\sim 2 \text{ mm a}^{-1}$, on the Yakapınar-Göksun Fault: the difference being taken up by distributed deformation within the northern "promontory" of the African plate, which appears to involve a combination of anticlockwise rotation and distributed left-lateral simple shear. It is proposed that this boundary first developed at the same time as the NAFZ, but its original geometry involving left-lateral slip on the Karataş-Osmaniye Fault has since become locked by the presence of relatively strong ophiolitic crust within this fault zone. The kinematic consistency of this model requires one to relax the assumption that brittle upper crust and mantle lithosphere are moving in step, consistent with the assumed presence of a weak layer of lower crust in between. The development of the NAFZ during the Messinian can thus be explained as a consequence of a combination of forces resulting from (a) shear tractions applied to the brittle upper crust of Turkey as a result of relative westward motion of mantle lithosphere, caused by the pre-existing relative motions between the African and Arabian plates during the earlier Miocene; and (b) the reduction in normal stress and increase in right-lateral shear stress that resulted from the dramatic water unloading during the Messinian desiccation of the Mediterranean basin. Analysis indicates that this mechanism requires the effective viscosity of the lower crust of Turkey to be $\sim 5 \pm 3 \times 10^{19} \text{ Pa s}$, consistent with recent estimates in other localities. The well-documented near-total absence of internal deformation within the Turkish plate thus does not result from high strength: it results from the geometry of its boundaries which allow them to slip without any need for internal deformation. The main imperfection in this pattern of boundaries results from the high-strength "patch" on the Turkey-Africa plate boundary in southern Turkey. The seismicity in this locality appears correlated with major earthquakes on the NAFZ, suggesting the possibility that this boundary behaves as a "geometrical lock" whose slip, in moderate-sized earthquakes, can permit much larger amounts of slip in much larger earthquakes on the NAFZ. Future detailed monitoring of this region may thus provide the basis for a system of advance warning of future destructive earthquakes on the NAFZ.

Key Words: Turkey, Syria, Israel, Lebanon, North Anatolian Fault Zone, East Anatolian Fault Zone, Dead Sea Fault Zone, plate kinematics, crustal rheology, lower-crustal flow, Quaternary, Pliocene, Messinian

Ortadoğu ve Doğu Akdeniz'in Güncelleştirilmiş Kinematığı

Özet: Akdeniz ve Orta Doğu bölgelerinin günümüzdeki görelî levha hareketleri için, jeoloji ve GPS verilerine dayalı olarak gözden geçirilmiş, kendi içinde tutarlı, sayısal bir kinematik model ortaya konmuştur. Güney Ölü Deniz Fay Zonu kesimindeki Afrika ve Arap levhalarının kırılğan üst kabuğunun görelî hareketleri $31.1^{\circ}\text{N } 26.7^{\circ}\text{E}$ Euler kutubunda, $0.278^{\circ}\text{My}^{-1}$ lık bir görelî dönmeyle temsil edilmektedir. Ölü Deniz Fay Zonu'nda (ÖDFZ) ortaya çıkan tahmini hareket hızı 4.0 mm/yıl dır. Kuzey ÖDFZ'nun kinematığı aşağı yukarı aynı Euler kutubuna sahiptir fakat $0.243^{\circ}\text{My}^{-1}$ lık bir görelî dönme gösterir. Bu farkın sebebi görelî hareketin küçük bir bileşeninin Palmyra kıvrım kuşağı'nda oluşturduğu kısalmadır. Suriye ve güney Türkiye'deki kuzey ÖDFZ, transpresiyonel sıçrama serisi olarak kabul edilir. Burada sol yanall atımın hızı, bu atım komşu levhalar arasındaki görelî harekete verev konumlu olduğu için görelî levha hareketi hızından oldukça düşüktür. Bu geometri, kısmen kuzey ÖDFZ'nun bazı kollarının levha hareketine uygun yönelimde olmadığı halde eski fay segmentlerini tekrar harekete geçirmesi ve kısmen de Levant kıyı şeridinin kuzeybatıda Kıbrıs'a doğru devamı olması gereken ÖDFZ'nun ideal ilksel geometrisinin bu hat boyunca varolan yüksek dirençli kabuk tarafından engellenmesi neticesinde meydana gelmiştir. Doğu Anadolu Fay Zonu (DAFZ) için belirlenen atım hızı $\sim 8\text{ mm/yıl}$ dır. Bu hız ile gözlenen toplam atım birarada değerlendirildiğinde, ÖDFZ'nun yaşının $\sim 4\text{ My}$ olması gerekmektedir. ÖDFZ oluşmadan önceki Malatya-Ovacık Fay Zonu üzerindeki atımı kapsayan bir önceki deformasyon fazı $\sim 7-4\text{ My}$ olarak yaşlandırılmıştır, bu da Kuzey Anadolu Fay Zonu'nun (KAFZ) oluşum zamanının daha önce düşünüldüğü gibi $\sim 5\text{ My}$ değil $\sim 7\text{ My}$ olduğunu gösterir. Batı KAFZ'daki yerel kanıtlar da $\sim 7\text{ My}$ veya Erken Messiniyen yaşını desteklemektedir. KAFZ'nun günümüzdeki ayrıntılı kinematığı Türk ve Avrasya levhaları arasındaki $30.7^{\circ}\text{N } 32.6^{\circ}\text{E}$ merkezli $1.2^{\circ}\text{My}^{-1}$ lik görelî dönmeyle de içerecek şekilde GPS kullanarak 2000'de belirlenmiş olan Euler vektörü ile belirlenmiştir. Bu Euler vektörü, levhalar arasında 25 mm/yıllık bir görelî hareketi öngörür; aynı zamanda KAFZ'nin çevresinde de saçılmış bir sağ yanall basit makaslama bileşenin varlığını gösterir. Türkiye ve Afrika levhaları arasındaki görelî sol yanall hareket için tahmin edilen hız $\sim 8\text{ mm/yıl}$ olarak belirlenmiştir. Ancak, bu sınırın karadaki kısmının yerel sol yanall atım hızı Yakapınar-Göksun Fayı üzerinde sadece 2 mm/yıl olarak hesaplanmıştır; aradaki fark, saatin tersi yönünde bir dönme ve saçılmış basit sol yanall makaslamanın birlikte etkilediği Afrika levhasının kuzeye devamının da içinde bulunduğu yayılmış deformasyon tarafından alınmıştır. Bu sınırın ilk önce KAFZ ile aynı zamanda geliştiği, fakat Karataş-Osmaniye Fayı'ndaki sol yanall atımı da içeren orjinal geometrisinin bu fay zonu içindeki görelî olarak dirençli ofiyolit kabuğunun gelişimiyle kilitlendiği öne sürülmektedir. Bu modelin kinematik tutarlılığı, aralarında zayıf bir alt kabuk katmanı bulunduğu kabulü ile uyumlu olarak, kırılğan üst kabuk ile manto litosferinin aşamalı hareket etmesini gerektirir. Böylece KAFZ'nun Messiniyen'deki gelişimi bir dizi kuvvetin birleşmesiyle açıklanabilir; (a) Erken Miyosen'de Afrika ve Arap levhaları arasındaki önceden varolan görelî hareketler nedeniyle manto litosferinin görelî batıya hareketinin bir sonucu olarak makaslama gerilmelerinin Türkiye'deki üst kırılğan kabuğa uygulanması, (b) Akdeniz havzasının Messiniyen'deki kuruması esnasında suyun boşalması sonucu normal gerilmedeki azalma ve sağ yanall makaslama gerilmesindeki artış. Yapılan analizler, diğer alanlardaki son hesaplamalarla uyumlu biçimde bu mekanizmanın çalışması için Türkiye'nin alt kabuğunun etkin viskozitesinin $\sim 5\pm 3\times 10^{19}\text{ Pa s}$ olması gerektiğini göstermektedir. Bu yüzden Türkiye levhasının içsel deformasyonun iyi belgelenmiş verilerinin olmaması yüksek dayanımlılıktan kaynaklanmamaktadır, iç deformasyona ihtiyaç duymadan kaymalarını sağlayan sınır geometrilerinden kaynaklanmaktadır. Bu sınır modelindeki ana eksiklik Güney Türkiye'de Türkiye-Afrika levha sınırındaki yüksek dayanımlı "yama"dan doğmaktadır. Bu alandaki sismisite KAFZ üzerindeki büyük depremlerle korole edilebilir görülmektedir. Bu sınırın olası bir "geometrik kilit" gibi davranmasından dolayı orta büyüklükteki depremlerdeki atımının KAFZ üzerinde daha büyük depremlerde daha fazla miktarda atıma izin vermesi mümkündür. Bu bölgenin önümüzdeki dönemlerde detaylı izlenmesiyle KAFZ üzerinde gelecekte meydana gelebilecek yıkıcı depremler için gelişmiş bir uyarı sisteminin temelini oluşturabilir.

Anahtar Sözcükler: Türkiye, Suriye, İsrail, Lübnan, Kuzey Anadolu Fay Zonu, Doğu Anadolu Fay Zonu, Ölü Deniz Fay Zonu, levha kinematığı, kabuk reolojisi, alt-kabuk akışı, Kuvaterner, Pliyosen, Messiniyen

Introduction

Active crustal deformation within and around Turkey reflects the interaction between the Eurasian, African, Arabian, and Turkish plates (Figure 1). The Turkish plate (TR) is bounded to the north by the right-lateral North Anatolian Fault Zone (NAFZ), which separates it from Eurasia (EU), and to the south and west by the active plate margin formed by the Hellenic and Cyprus trenches, along which the African plate (AF) is subducting northward. The NAFZ dies out southwestward into a zone of distributed crustal extension within the Aegean

region, overlying the Hellenic subduction zone. The eastern boundary of the Turkish plate is a complex left-lateral strike-slip fault zone, adjoining both the African and Arabian (AR) plates. The TR-AR plate boundary follows the left-lateral East Anatolian Fault Zone (EAFZ), which splays southwestward in SE Turkey into the TR-AF and AF-AR plate boundaries, the latter being known as the Dead Sea Fault Zone (DSFZ).

Westaway (1994a) published the first internally consistent quantitative overall kinematic model for this region, which constrained the senses and rates of slip on

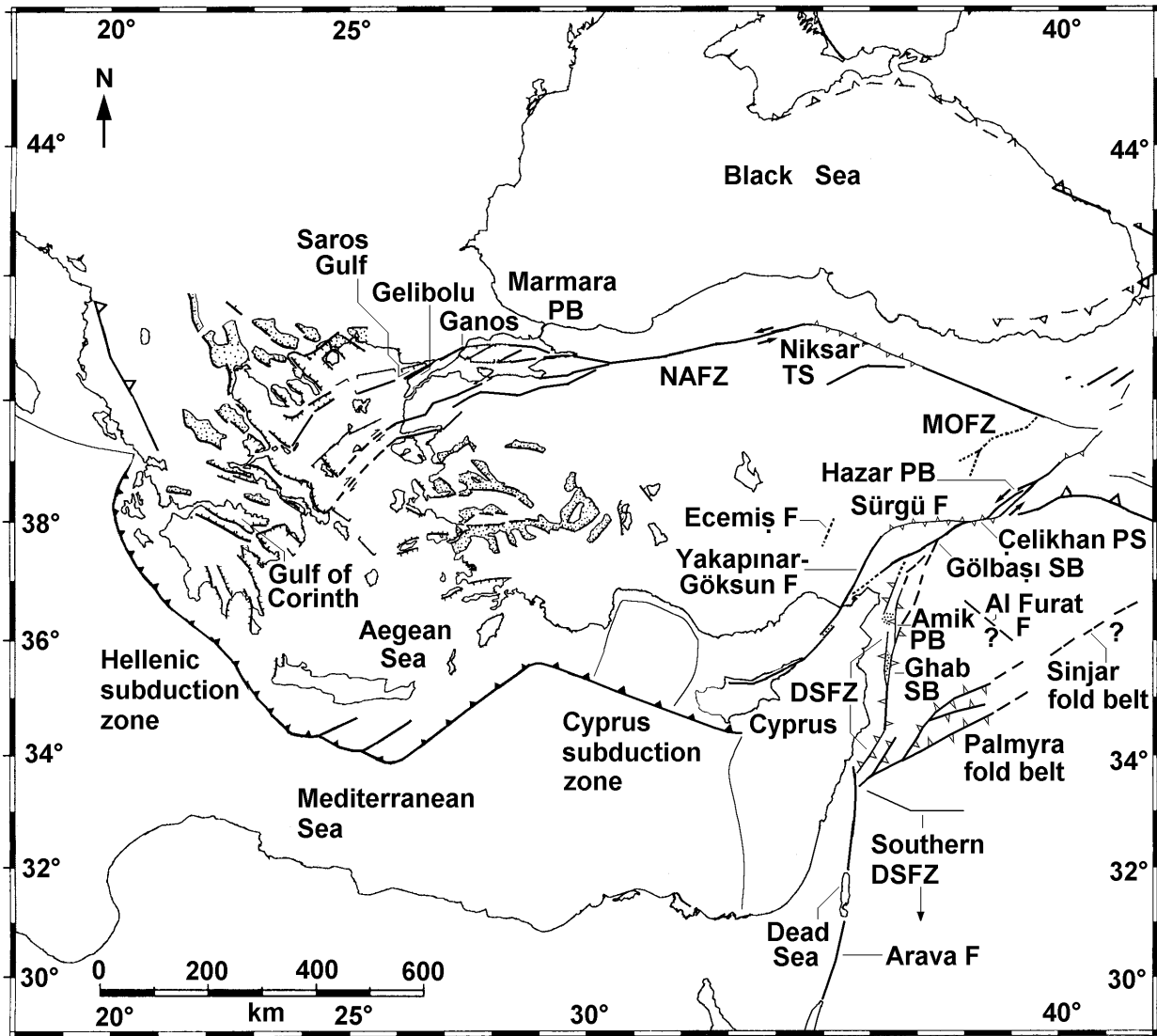


Figure 1. Map of the present study region. Fault geometry is summarised from Westaway & Arger (1996, 2001), McClusky *et al.* (2000), Westaway (2002b), and this study. The Al Furat Fault and Sinjar fold belt, possible continuations of the active crustal deformation in the Palmyra fold belt involving NW–SE left-lateral slip and/or NW–SE shortening, are summarised from Lovelock (1984). The North Aegean Trough (e.g., Le Pichon *et al.* 1984) marks the southwestward continuation of the northern strand of the NAFZ offshore of Saros Gulf.

each of these fault zones individually using appropriate local evidence and then demonstrated the overall kinematic consistency of the scheme. This approach superseded other investigations, such as Jackson & McKenzie (1998), who determined slip rates on individual fault zones in this region without regard for their overall consistency, or Dewey *et al.* (1986) and Karig & Kozlu (1990), who determined qualitative kinematic models for the senses (but not the rates) of

crustal deformation. Part of the point of the Westaway (1994a) study was to provide a “benchmark” kinematic model using geological data, for comparison with direct geodetic measurements of rates and senses of crustal deformation in this region using the Global Positioning System (GPS), which were then in their early stages. This model has indeed been used as such in the subsequent literature reporting GPS results (e.g., Straub *et al.* 1997; Reilinger *et al.* 1997; McClusky *et al.* 2000; Kahle *et al.*

2000). Another reason behind the Westaway (1994a) study was to assess the relative strengths of different aspects of the available evidence, to determine where future investigations could be most usefully targeted to improve constraint on senses, rates and time-scales of crustal deformation using geological evidence. Subsequent studies of mine (e.g., Westaway 1994b, 1995a, 1996, 1998, 1999b, 2002, 2003; Westaway & Arger 1996, 2001; Mitchell & Westaway 1999; Arger *et al.* 2000; Yurtmen & Westaway 2001a, b; Yurtmen *et al.* 2002; Westaway *et al.* 2002a, b; Bridgland *et al.* 2002) have kept this aim in mind. On the same time-scale, many other people have of course also investigated this topic. Some of these studies (e.g., Tüysüz *et al.* 1998; Armijo *et al.* 1999) have provided fundamentally important new evidence, whereas others (in many cases discussed in the references cited above) have proposed models – involving revisions to the regional kinematics – that contradict established evidence. For instance, some recent studies have proposed that the Ecemiş Fault in central-southern Turkey (Figure 1) is slipping at such a high rate that it should be considered on a par with the NAFZ and EAFZ – a view that can be emphatically contradicted (e.g., Westaway 1999b, 2002a), as radiocarbon dating evidence (Çetin 2000) constrains its slip rate to ~ 0.03 mm a⁻¹. As a result, no attempt is made here to review every such contribution to the literature. To keep this study focused and of manageable length, I will instead concentrate on new data that – in my opinion – contributes usefully to improving constraint on the regional kinematics.

On the same time scale, it has gradually become clear – through my own work both in Turkey and elsewhere (e.g., Westaway 1994b, c, 1995b, 1996, 1998, 1999a, 2001, 2002b, c, d, e; Mitchell & Westaway 1999; Westaway *et al.* 2002a, b) and the work of other people – that in regions of continental crust of normal thickness and geothermal gradient, the plastic lower crust is sufficiently weak (i.e. has sufficiently low viscosity) that it is able to flow significantly relative to the overlying brittle upper crust and/or the underlying mantle lithosphere. It now indeed seems essential to consider the weakness of the lower crust when explaining many aspects of the geological evolution of Turkey and its surroundings (e.g., Westaway 1994b, 1996, 1998, 2002b; Mitchell & Westaway 1999; Westaway *et al.* 2003). The acceptance that the lower crust is so weak demands that one take

into account the possibility that blocks of the brittle upper crust can move relative to the underlying mantle lithosphere (e.g., Westaway 1995b). The existence of *vertical* motions of the brittle layer relative to the underlying mantle lithosphere, due to net inflow or outflow of lower crust, has featured in some recent investigations of Turkey and its surroundings (e.g., Mitchell & Westaway 1999; Arger *et al.* 2000; Westaway 2002b; Westaway *et al.* 2003). However, the possibility of significant *horizontal* relative motions between the upper crust and mantle lithosphere has not been considered in any previous regional kinematic model for Turkey. Of course, any region of continental crust may contain localities where the crust is stronger than usual: possibly because it contains mafic material (e.g. ophiolite) that does not flow significantly at the temperatures encountered (e.g., Westaway 1995b); or possibly because the continental crust is locally thin and thus brittle to the Moho, lacking any significant weak lower-crustal channel (e.g., Westaway 2001). As will become clear, this property of the crust now also seems essential for understanding the regional kinematics of Turkey.

The aims of the present study are thus, first, to highlight new evidence that adds to the constraint on the regional kinematics of Turkey. Second, is to obtain updated estimates for the senses and rates of slip on major fault zones that are consistent with both the GPS data and the available geological evidence. Third, is to interpret the resulting pattern of regional deformation in terms of the kinematics of the brittle upper crust and mantle lithosphere and the relative horizontal motions between them. Fourth, is to discuss implications of this new kinematic model for the dynamics of this region. This includes consideration of the mechanical reasons for why the present geometry of faulting involving the NAFZ developed in the first place, and the possibility of earthquake triggering between fault zones.

The Dead Sea Fault Zone

The DSFZ consists of a N-S trending southern segment, which bounds Israel and Jordan and links southward to the oceanic spreading centre in the Red Sea, a central segment oriented towards N30°E across Lebanon, and a northern segment that is oriented N-S across Syria but bends towards the NNE and splays into a complex array

of en-echelon fault strands (Figure 2) in southeast Turkey. The total slip on the DSFZ has been estimated as ~105 km in the south (e.g., Freund *et al.* 1970; Garfunkel 1981; Quennell 1984) and ~70–80 km in the north (e.g., Freund *et al.* 1970; Dewey *et al.* 1986). The ~105 km estimate in the south is based on matching many independent features across the southern DSFZ. In contrast, the ~70–80 km estimate in the Turkey-Syria border region is based on projecting the southern outline of outcrops of the Hatay/Baer-Bassit ophiolite on the African side (K-L in Figure 3) into the line of the DSFZ in the Orontes valley (to the north of I in Figure 3), and matching it against the southern margin of the ophiolite farther north on the Arabian side, around locality C (Figure 3). Heimann (2001) has suggested that this estimate of total slip based on projection is contentious: a small change in the projection angle can reduce the estimate by many tens of kilometres. Furthermore, as Yurtmen *et al.* (2002) have noted, this estimate excludes the slip on the Afrin Fault that runs east of the Hatay ophiolite (Figures 2 & 3): it only covers the en-echelon Amanos and East Hatay faults. In addition, although this southern margin of the ophiolite directly abuts the East Hatay Fault to the east, south of Tahtaköprü (C in Figure 3), its supposed counterpart – west of the DSFZ SE of Antakya (K-L in Figure 3) – is separated from the fault strand by a zone (~10–20 km wide) of younger outcrop (Figure 3). This ophiolite outcrop is indeed sufficiently far from the DSFZ that associating it with any specific outcrop on the opposite side seems arbitrary. The southernmost points where ophiolite crops out directly adjacent to the western margin of the DSFZ are around the SW corner of the Amik Basin north and northeast of Antakya (e.g., G or H in Figure 3). The southernmost point where ophiolite crops out immediately east of the Amanos Fault was identified by Yurtmen *et al.* (2002) as between the villages of Bektaşlı and Dokuzlar (see also Atan 1969; Figures 2 & 3), some ~45–50 km farther north (F in Figure 3). Yurtmen *et al.* (2002) suggested that the East Hatay Fault could have slipped by ~15 km based on the N–S separation of the southernmost serpentinite outcrops on either side of it (D-C1 in Figure 3). Better estimates can instead be obtained from the N–S offset measured between locality D, just inside Syria on the Africa side of the East Hatay Fault, and locality C on the Arabian side. The southern margin of serpentinite is offset ~10 km (E1-C1 in Figure 3), as is the southern margin of radiolarian chert located ~3 km farther south

(Eo-Co in Figure 3). The combined slip on the Amanos and East Hatay faults may thus be as little as ~55 km. The component of slip on the Afrin Fault farther east remains unknown.

To check this ~55 km estimate, investigations have been made of the structure and lateral facies variations in the Mesozoic and Tertiary rocks exposed in the Amanos Mountains between Kırıkhan and Hassa and in the uplands to the west of Gaziantep (e.g., Atan 1969; Terlemez *et al.* 1997). Although some broadly equivalent features have been identified, how to project them onto the line of the fault zone to establish them as piercing points remains problematic. I thus do not discuss this evidence further at this stage. It is nonetheless evident that the northern DSFZ could readily have slipped by many tens of kilometres, but probably tens of kilometres less than the southern DSFZ has slipped.

Inspection of Figure 3 also indicates other possible piercing points giving measurements of apparent slip. East of Yalankoz, just inside Syria, the southern margin of an outcrop of Late Jurassic limestone is offset left-laterally by ~3 km (M in Figure 3). The southern margin of outcrop of Pliocene marine sediment in the Orontes valley is offset left-laterally by ~10 km (I-J in Figure 3). This marine sediment formed in the earliest Pliocene, when the Mediterranean Sea briefly flooded this area (e.g., Ponikarov *et al.* 1967) following the Messinian regression (e.g., Ryan & Cita 1978) that ended at 5.3 Ma. At both these suggested piercing points, the southern margin of the marine sediment outcrop marks the southward limit beyond which this sediment has not yet been eroded. As in any such instance, differential erosion would thus mean that the true amount of left-lateral slip is not being expressed (e.g., Westaway 1999b). Nonetheless, ~10 km of slip since ~5.3 Ma would imply a left-lateral slip rate of ~1.9 mm a⁻¹, roughly what is expected from the regional kinematics and roughly what is observed on the Amanos Fault farther north (from offsets of Quaternary basalts at localities A and B in Figure 3) (see below).

The age of the DSFZ has been estimated in many studies as ~15–19 Ma (e.g., Garfunkel 1981; Ginat *et al.* 1998). The upper age bound of 19 Ma exists because basaltic dykes of this age exposed in Sinai are offset by the full ~105 km distance from their counterparts east of the DSFZ in Jordan (e.g., Eyal *et al.* 1981; Steinitz *et al.* 1981). The age of the central and northern DSFZ has



Figure 2. Map of significant fault segments of the TR-AR and TR-AF plate boundaries linking southeast Turkey, Lebanon, and Cyprus, in relation to GPS points, from McClusky *et al.* (2000). Faults in Lebanon and southern Syria are from Ponikarov *et al.* (1966) and Walley (1998). Those in northern Syria are from Ponikarov (1966) and the analysis in this study. Faults in and offshore of southern Turkey are from Aksu *et al.* (1992a, b), Westaway & Arger (1996), Terlemez *et al.* (1997), Coşkun & Coşkun (2000), Yurtmen & Westaway (2001b), Yurtmen *et al.* (2002), and the analysis in this study. The three “problematic faults” shown are the NE continuation of the Serghaya Fault across the Homs area of Syria, from Walley (1998), which – if it exists – appears to have not been active since at least the Early Pliocene (see Figure 4 and its caption), the NW end of the Al Furat Fault (Lovelock 1984), which is discussed in the text, and the “Kartal Fault” of Westaway & Arger (1996) in southern Turkey, which is a misinterpretation.

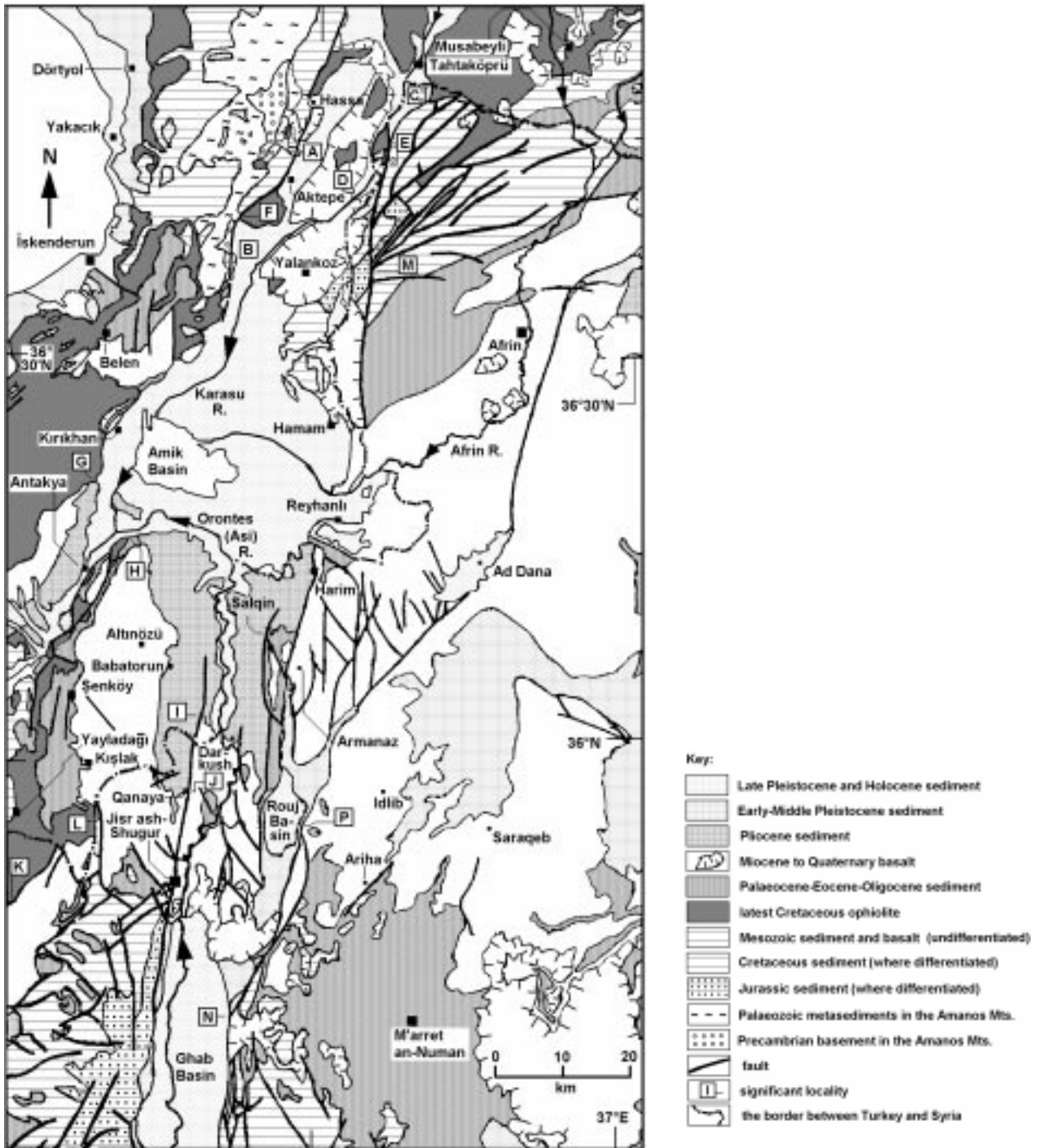


Figure 3. Maps of possible piercing points across the northern DSFZ. Adapted from Tolun & Erentöz (1962) and Ponikarov *et al.* (1966). Some detail in Syria should be regarded as tentative, as details conflict between the Ponikarov *et al.* (1966) map and either Figures in the Ponikarov *et al.* (1967) guide or later references. See text for discussion.

instead proved controversial. Some studies (e.g., Freund *et al.* 1970; Dewey *et al.* 1986; Westaway 1994a; Yurtmen *et al.* 2002) have assumed that it formed at the same time as the southern DSFZ and has continued to slip to the present day. Others (e.g., Girdler 1990; Butler *et al.* 1997, 1998; Butler & Spencer 1999) have suggested that it formed at the same time as the southern DSFZ but (notwithstanding its obvious historical seismicity) ceased to be active sometime around the Late Miocene when slip migrated onto another (hypothetical) fault zone located offshore to the west. Others (e.g., Brew *et al.* 2001; Heimann 2001) have suggested in contrast that the northern DSFZ did not become active until the Early Pliocene. Simple fieldwork in western Syria (see below) allows one to distinguish between these contradictory hypotheses, in favour of the first one.

The Westaway (1994a) kinematic model assumed (1) that both N-S-trending segments of the DSFZ are transform faults and (2) the slip rate on these segments can be estimated by dividing the ~105 km total slip by the ~15 Ma estimated age to obtain ~7 mm a⁻¹. The central segment through the mountains of Lebanon is of course a transpressive stepover with more complex kinematics (e.g., Westaway 1995a). The major revisions proposed in this study are (1) a substantially lower Plio-Quaternary slip rate (~4 mm a⁻¹) for the southern, transform-faulting, segment of the DSFZ and (2) the northern DSFZ is reinterpreted as another transpressive stepover (at a more acute angle than the Lebanon stepover) and not a transform fault zone.

This new ~4 mm a⁻¹ slip rate estimate for the southern DSFZ obtained in this study (see below) is, of course, less than the minimum possible overall time-averaged slip rate of ~105 km/~19 Ma or ~5.5 mm a⁻¹, suggesting that the DSFZ was slipping faster in the Miocene than at present. Later in this paper it is proposed that the regional kinematics are currently being “jammed” by the presence in the AF-TR plate boundary zone of relatively strong crust containing the Hatay ophiolite. This effect may have led to the regional kinematics adjusting at, say, ~4 Ma (see below), with the DSFZ slip rate reducing from, say, ~6 mm a⁻¹ (giving 90 km of slip between ~19 Ma and ~4 Ma) to the present ~4 mm a⁻¹. Ten Brink *et al.* (1999) have noted abundant evidence of small changes in the sense of slip along the southern DSFZ during its evolution, consistent with this and possibly other adjustments in the kinematics. However,

incorporating such fine detail into a kinematic model for the whole of the Middle East and eastern Mediterranean region is beyond the scope of this study.

The Arava Valley, Israel/Jordan

The southernmost DSFZ segment (~30–31°N, ~35°E; between the Dead Sea and the Gulf of Aqaba) is marked by a clear linear valley, which delineates the border between Israel and Jordan. Plio-Quaternary sediments are exceptionally well exposed in this region, as a result of the arid climate. Recent studies of these sediments provide improved constraints on the DSFZ kinematics.

Zhang (1998) noted Holocene stream channels and alluvial fan surfaces in this area that are offset left-laterally by 39 and 22.5 m, these offsets being radiocarbon dated to 8.5 and 4.7 ka, indicating a slip rate of ~4.6–4.8 mm a⁻¹ on this time-scale. Zhang (1998) also noted an older alluvial fan, which post-dates the latest Pleistocene pluvial Lake Lisan (when the Dead Sea was greatly enlarged due to the wetter climate), offset by 54 m. He adopted a 12 ka age for the desiccation of this lake basin, thus indicating a slip rate of ~4.5 mm a⁻¹ on this time-scale, also. However, others (e.g., Kaufman *et al.* 1992) have proposed that it disappeared at ~15 ka, implying a lower slip rate of ~3.6 mm a⁻¹. Klinger *et al.* (2000) noted a range of other localities where the oldest post-Lake-Lisan alluvial fan deposits are offset left-laterally by 36±2 m. Taking a 12–15 ka age for these deposits would instead give a slip rate of ~2.3–3.2 mm a⁻¹.

Klinger *et al.* (2000) also noted a Late Pleistocene alluvial fan deposit, pre-dating Lake Lisan and offset left-laterally by ~500 m, which they cosmogenically dated (using ¹⁰Be) to 140±31 ka. They assumed that this deposit formed during the last interglacial [oxygen isotope stage (OIS) 5e; ~125 ka], thus giving a slip rate of ~4.0 mm a⁻¹. However, investigations of fluvial sediment transport in Syria by Bridgland *et al.* (2003) suggest that the most important sediment movements occur during glacial maxima, not interglacials. This fan could well thus have accumulated during OIS 6 (~140 ka), not OIS 5e, giving a slip rate of ~3.6 mm a⁻¹.

Ginat *et al.* (1998) noted a series of older alluvial fan deposits on the western (Israel) side of the Arava Valley, each offset left-laterally by ~15 km from its sediment source on the eastern (Jordan) side of the DSFZ,

indicating that no linear valley existed at the time. The age of these deposits is not well constrained, other than to the post-Middle Miocene. Ginat *et al.* (1998) accepted a Pliocene (~5–2 Ma) age for these offset alluvial fans, implying a slip rate of ~3.0 to 7.5 mm a⁻¹. Numerical modelling by Bridgland *et al.* (2003) indicates that western Syria (and presumably other parts of western Arabia, also) has experienced ~400 m of regional uplift since the start of the Pliocene, substantially adding to the relief. The uplift rate in western Syria increased substantially at ~3 Ma. If the associated increase in relief marked the time of disruption of this older drainage system, leading to the creation of the linear valley, then the subsequent slip rate can be estimated as ~5 mm a⁻¹. An alternative estimate can be obtained by noting that the regional kinematics adjusted in the Early Pliocene, when the EAFZ came into being (e.g., Westaway & Arger 1996, 2001). The time of this adjustment can be estimated by dividing its ~35 km of slip by its estimated slip rate of ~8 mm a⁻¹ (see below) and is ~4.4 Ma. If this adjustment caused the initiation of the Arava linear valley, possibly by creating a small component of transtension where none existed before, then the subsequent slip rate can be estimated as ~3.4 mm a⁻¹. As already noted, ten Brink *et al.* (1999) have identified abundant evidence of small changes in the slip sense along the DSFZ, so such a change – from pure left-lateral slip to a possible small component of transtension – is entirely reasonable.

Klinger *et al.* (2000) estimated the slip rate on the Arava segment of the DSFZ as 4 ± 2 mm a⁻¹. They also determined the Euler pole to the DSFZ as at 31.1°N 26.7°E using evidence from many localities on the boundaries of the Arabian plate, near the positions determined in many previous studies (e.g., Garfunkel 1981) using only local evidence from along the southern DSFZ. They also determined a rate of relative rotation of 0.396° Ma⁻¹, which yields a 5.7 mm a⁻¹ slip rate in the Arava Valley (30.8°N, 35.4°E). This rate seems too high: adopting instead a nominal local slip rate of 4.0 ± 0.5 mm a⁻¹ causes the rotation rate to adjust to 0.278 ± 0.035 ° Ma⁻¹. The resulting Euler vector (pole: 31.1°N 26.7°E, rotation rate 0.278° Ma⁻¹) will be used to describe the relative motions of the brittle upper crust of Africa and Arabia across the southern DSFZ. To describe the kinematics of the northern DSFZ, after allowing for the “absorption” of some of the northward motion of Arabia by shortening in the Palmyra fold belt (e.g., Chaimov *et*

al. 1990; see below), the same Euler pole is assumed but with a reduced rotation rate of 0.243° Ma⁻¹, equivalent to a 3.5 mm a⁻¹ slip rate on the southern DSFZ.

The Lebanon Steppover and Palmyra Fold Belt

Within Lebanon, the DSFZ is oriented towards N30°E, its main strand – which forms the western margin of the Bekaa Valley and the eastern flank of the Lebanon mountain range – being known as the Yammouneh Fault (e.g., Walley 1998). Other significant left-lateral fault segments are also present, notably the Serghaya Fault that forms the eastern margin of the Bekaa Valley and the western flank of the Anti-Lebanon mountains. On the southern part of this fault (around Zabdani to the NW of Damascus; Figure 2) the Holocene slip rate is estimated as ~1–2 mm a⁻¹ (Gomez *et al.* 2001). The surroundings to these faults are pervasively fractured by minor faulting, and folded (e.g., Westaway 1995a; Walley 1998). They are also tilted away from the Yammouneh Fault on both sides: in the escarpment adjacent to this fault, Jurassic and Cretaceous rocks are exposed, the Tertiary sequence formerly covering them having been eroded, this tilting dying out over distances of up to ~20 km, where the Tertiary sequence is preserved and exposed (e.g., Walley 1998).

Attempts at explaining the kinematics of this structure in terms of rigid blocks bounded by transform faults that are oriented oblique to the plate motion (e.g., Walley 1988) clearly do not work (e.g., Westaway 1995a). This led to the suggestion (Westaway 1995a) that the left-lateral faults within this structure are not transform faults: they are instead bounding blocks that are themselves deforming internally, this deformation including components of distributed left-lateral simple shear and/or distributed shortening. Westaway (1995a) obtained an algebraic solution for the velocity gradient tensor and deformation gradient tensor describing this situation, in which an internal strike-slip fault, within the structure, is slipping at a rate U and oriented at an angle θ to adjoining transform faults that are themselves oriented parallel to the motion of the adjoining plates and slipping at rate V . In addition to predicting all components of the model region's deformation, the most straightforward result from this analysis was a demonstration that the ratio U/V is limited by an upper bound, k , where

$$\cos(\theta) = k \equiv U / V \quad (1)$$

Numerous palaeomagnetic studies (results compiled by Westaway 1995a) indicate anticlockwise rotation within these surrounding mountain ranges by $\sim 30^\circ$ since the Early Cretaceous. Westaway (1995a) suggested that this rotation has resulted from distributed left-lateral simple shear across the Lebanon stepover during slip on the DSFZ. However, Walley (1998) contested this point: he argued instead that some aspects of the structure of this stepover region (including, presumably, the palaeomagnetic rotations) formed in the Late Cretaceous, during an earlier phase of crustal deformation that was unrelated to the DSFZ.

The parameters used in Westaway's (1995a) calculations require substantial revision in the light of new data. First, the new southern DSFZ Euler vector discussed earlier predicts (for a representative point within the Lebanon stepover, at 34.1°N , 36°E) that AF-AR motion is locally oriented towards $\text{N}18^\circ\text{W}$ at $\sim 4.5 \text{ mm a}^{-1}$. The angle θ between this motion direction and the $\text{N}30^\circ\text{E}$ strike of the Yammouneh Fault is thus 48° , not the 32° calculated by Westaway (1995) using Garfunkel's (1981) Euler pole. Second, Walley (1998) showed from the offset of distinctive Cretaceous inliers used as piercing points that the Yammouneh Fault has slipped left-laterally by 47 km, and estimated a further ~ 20 km of slip on the Serghaya Fault. The ratio of this 67 km of slip to the 105 km on the southern DSFZ indicates that k [equation (1)] is ~ 0.64 . This is very close to $\cos(48^\circ)$ or ~ 0.67 , suggesting that the left-lateral faults in the Lebanon stepover have slipped by about the maximum distance permitted by its geometry. Westaway (1995) instead assumed, following Hancock & Atiya (1970), that the Yammouneh Fault has slipped only ~ 7 km.

In terms of Westaway's (1995a) notation, ψ for the Lebanon stepover is thus 48° , and the initial and final orientations of the Early Cretaceous magnetisation vectors require α_0 50° and α 80° . Westaway's (1995a) equation (A31) allows one to estimate from these parameters the total shortening strain ζ in the Lebanon Mountains that would be required to account for the observed $\sim 30^\circ$ anticlockwise rotation. With the above parameter values, it requires ζ to be ~ 12 , an implausibly high value, rather than the geologically more plausible value of ~ 2 deduced by Westaway (1995a). Walley's (1998) intuitive conclusion, that such large rotations cannot have been associated with slip on the DSFZ, is thus entirely supported by the new data. Westaway's (1995a)

analysis indeed indicates that, in the limit of k being as large as possible, the strain rate for distributed simple shear across a stepover is zero. Structural trends (or embedded magnetisation vectors) can still experience some rotation, due to the flattening effect of the component of distributed shortening perpendicular to the line of the stepover: but any resulting rotation is likely to be small. It is presumed that this component of distributed crustal shortening is being accommodated by thickening of the brittle upper crust, requiring surface uplift. However, as a result of this surface uplift, the upper part of the crustal column is presumed to have been eroded, thus explaining why older rocks are typically exposed along the Lebanon stepover (e.g., Walley 1998). Their observed typical outward tilting can also be readily explained as a consequence of a tapering in the crustal shortening strain rate away from the DSFZ.

The Palmyra fold belt evidently remains active at the present day: seismicity maps (e.g., McClusky *et al.* 2000; Figure 1) indicate that its instrumental seismicity in recent decades involves occasional moderate-sized (magnitude $M > 5.0$) earthquakes, with focal mechanisms consistent with left-lateral slip on faults oriented SW-NE. This region's long historical seismicity record reveals occasional much larger events, such as on 21 August 1042 ($M \sim 7.2$) when Palmyra city was destroyed (e.g., Willis 1928; Ben-Menahem 1981). Ben-Menahem (1981) estimated from seismic moment summation for the available historical record that the resulting rate of left-lateral slip on this structure is $\sim 0.64 \text{ mm a}^{-1}$: although the sparseness of the available record and the difficulty of accurately estimating the size of historical earthquakes from the dimensions of macroseismic effects in such a sparsely populated desert region make any such estimate liable to considerable uncertainty. However, as the predicted plate motion is oriented at $\sim 60^\circ$ to this strike-slip faulting, using equation (1) the local rate of relative motion can be estimated from Ben-Menahem's (1981) result as $\sim 0.64 \text{ mm a}^{-1} / \cos(\sim 60^\circ)$ or $\sim 1.3 \text{ mm a}^{-1}$.

Walley (1998) proposed that the estimated ~ 20 km of left-lateral slip on the Serghaya Fault dies out in distributed shortening across the Palmyra fold belt farther north and east in Syria. Estimates of the total shortening within this fold belt range from ~ 20 km (Chaimov *et al.* 1990) to ~ 30 km (Khair *et al.* 1997). However, Walley (1998) argued that, as in Lebanon, some of the structure of the Palmyra fold belt pre-dates

the DSFZ, so the total of syn-DSFZ shortening in it is less. The DSFZ kinematic model proposed in this study is consistent with shortening at $\sim 0.69 \text{ mm a}^{-1}$ towards N18°W across the Palmyra fold belt, at a representative point at 34.8°N, 38°E, predicting $\sim 13 \text{ km}$ of shortening since $\sim 19 \text{ Ma}$.

It is likely that future constraint on the rate of shortening across the Palmyra fold belt and the sense of distributed deformation across the Lebanon stepover will come from GPS. However, no GPS solutions for the motion of any points in these regions have yet been published.

The Homs area, Western Syria

The DSFZ segment north of the Lebanon-Syria border, for which the name Masyaf Fault is suggested, trends almost due north (Figure 4), transecting the outcrop of Homs Basalt. Butler *et al.* (1997) reported K-Ar dates for the basalt cropping out along the Wadi Chadra valley, just south of the southern end of this fault in northernmost Lebanon, of $5.7 \pm 0.5 \text{ Ma}$ for the lower flow unit (pillowed) and $5.2 \pm 0.2 \text{ Ma}$ for the upper flow unit that erupted subaerially. Much of the upland land surface between Homs and the DSFZ, at altitudes of up to $\sim 1100 \text{ m}$, is covered by the Homs Basalt (Figure 4). Samples of this basalt from west of Homs have been K-Ar dated to $5.1 \pm 0.1 \text{ Ma}$, $5.4 \pm 0.1 \text{ Ma}$, and $5.5 \pm 0.1 \text{ Ma}$ (Mouty *et al.* 1992) (Figure 4). West of the DSFZ in northernmost Lebanon (Figure 4), Butler & Spencer (1999) have reported additional K-Ar dates of $6.7 \pm 0.2 \text{ Ma}$ and $5.7 \pm 0.7 \text{ Ma}$ for pillow basalt in the Wadi Chadra valley, and $6.5 \pm 0.2 \text{ Ma}$ for columnar-jointed basalt directly overlying this pillow basalt. They also reported dates of $\sim 5.5 \pm 0.2 \text{ Ma}$ and $5.2 \pm 0.2 \text{ Ma}$ for the youngest preserved basalt at Aandqat, $\sim 1 \text{ km}$ farther north and $\sim 150 \text{ m}$ higher up the stratigraphic section. Farther north at Mallouaa, just inside Syria, Mouty *et al.* (1992) reported another date, of $8.5 \pm 0.8 \text{ Ma}$ from just west of the DSFZ (Figure 4). A Late Miocene to earliest Pliocene age is thus indicated for this volcanism.

Walley (1998) has suggested that, in addition to the Masyaf Fault located SW and west of Homs, the Serghaya Fault continues NNE from the Bekaa Valley of Lebanon, into Syria: past Al Qusayr and SE of Homs, before splaying in the vicinity of Furqlus and Abu Qatur (Figure 2) into the Jhar and Bishri faults within the Palmyra fold

belt. However, geological mapping in the vicinity of Al Qusayr (e.g., Kozlov *et al.* 1963; Ponikarov *et al.* 1967) has revealed no evidence of any such fault (Figure 4), and none has been noted during recent fieldwork in this area (Bridgland *et al.* 2003), either. Nonetheless, most outcrop in this area is Pliocene and Quaternary (e.g., Dubertret & Vautrin 1938; Bourcart 1940; De Vaumas 1957; Van Liere 1961; Kozlov *et al.* 1963), and so it is conceivable that such a fault could have been active in the Miocene but slip on it has since ceased. However, the established geological mapping of Syria (e.g., Ponikarov *et al.* 1967) instead shows the Jhar and Bishri faults linked to the DSFZ a long way farther south: in the Syria-Lebanon border area SW of Damascus (Figure 2). It thus seems likely instead that the active slip on the Serghaya Fault gradually dies out northward within the Lebanon stepover, from its $\sim 1\text{--}2 \text{ mm a}^{-1}$ slip rate in the south (Gomez *et al.* 2001), and does not continue northeastward into Syria (contra Walley 1998).

Previous studies (e.g., Westaway 1994a, 1995a; Brew *et al.* 2001) have assumed that the Masyaf Fault is a transform fault segment. However, the structure of the DSFZ in Syria is similar (albeit on a smaller scale) to that in Lebanon: Cretaceous and Jurassic rocks are exposed along the Masyaf Fault (Figure 4). They also tilt away from it on both sides (Figures 4 & 5), although this tilting is asymmetric: it persists for $> \sim 40 \text{ km}$ to the west (Figure 5), but dies out within $\sim 20 \text{ km}$ to the east. Furthermore, the Homs Basalt is deposited on an erosion surface that is now tilted away from the DSFZ (Figure 5), in the same sense as but at a lower angle than the underlying structure is tilted. It can be presumed that this surface was subhorizontal at the time of basalt eruption: thus, much of the structural tilting occurred before $\sim 5 \text{ Ma}$ but some of it has occurred since, suggesting (by analogy with Lebanon) that this tilting is the result of distributed crustal shortening and thickening at a rate that decreases away from the DSFZ. By analogy with Lebanon, it can thus be argued that this part of the DSFZ is also a stepover – although at a more acute angle than in Lebanon. This interpretation is consistent with the revised DSFZ Euler vector, which requires relative plate motion towards N21°W in this part of Syria.

West of Homs (at 34.7°N, 36.35°E), the proposed northern DSFZ kinematic model predicts AF-AR relative motion at 4.16 mm a^{-1} towards N21°W, consistent with $\sim 79 \text{ km}$ of relative plate motion since 19 Ma. This

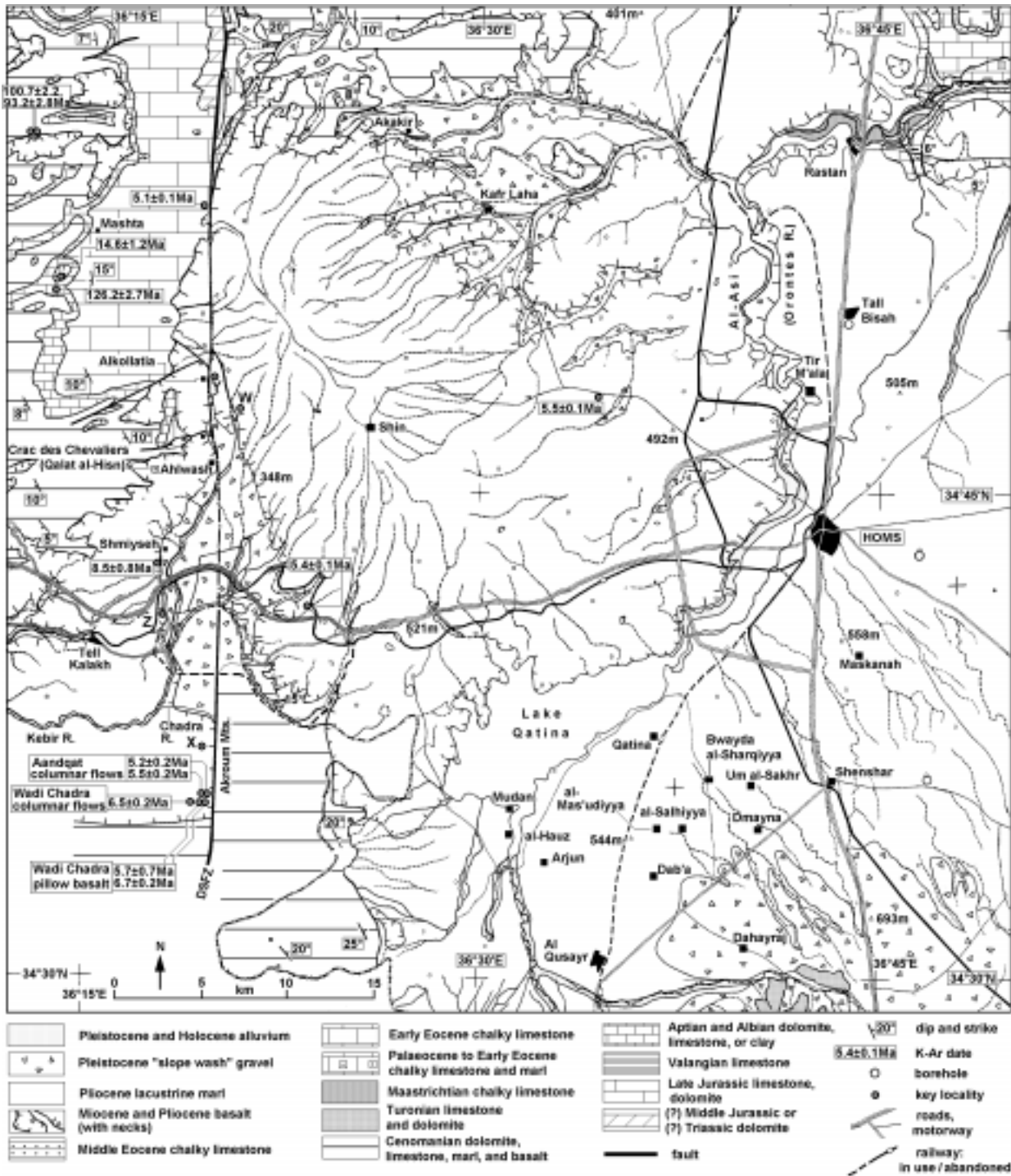


Figure 4. Geological map of the DSFZ and its surroundings in western Syria and northern Lebanon, adapted from Kozlov *et al.* (1963). Geological detail in Lebanon is simplified from Butler *et al.* (1997). K-Ar dates and site positions in Lebanon are from Butler & Spencer (1999). Those in Syria are from Mouty *et al.* (1992), the sites being located as accurately as possible using their map (their Figure 1b) rather than their table of coordinates, which in some cases do not tally with the map. The borehole shown directly east of Homs revealed basalt beneath 119 m thickness of Pliocene lacustrine marl. Approximate alignments of the modern road and railway networks have been added to facilitate location. The northward continuation of the Serghaya fault according to Walley (1998) (dotted line in Figure 2) runs SW-NE along the NW margin of the range of hills in Cretaceous limestone south of Dahayraj, and is then projected farther NE across the Pliocene marl outcrop depicted on this map.

requires a slip rate no greater than $4.16 \text{ mm a}^{-1} \times \cos(21^\circ)$ or 3.88 mm a^{-1} on the Masyaf Fault, predicting (if the same rate has been maintained) $\sim 19 \text{ km}$ of slip since 5 Ma and $\sim 74 \text{ km}$ of slip since 19 Ma. The 47 km of left-lateral slip on the Yammouneh Fault estimated by Walley (1998) requires, from earlier discussion, $47 \text{ km} / \cos(48^\circ)$ or $\sim 70 \text{ km}$ of relative motion between the adjoining plates, suggesting a $\sim 3.70 \text{ mm a}^{-1}$ time-averaged rate of relative motion. This requires a slip rate no greater than $3.70 \text{ mm a}^{-1} \times \cos(21^\circ)$ or 3.45 mm a^{-1} on the Masyaf Fault, predicting $\sim 17 \text{ km}$ of slip since 5 Ma and $\sim 66 \text{ km}$ of slip since 19 Ma. The very close similarity between these two independent sets of estimates suggests that the regional kinematics are now quite tightly constrained. The small mismatch could result from having underestimated the shortening across the Palmyra fold belt (see below) or having omitted any contribution to the relative plate motion from any other left-lateral fault within the Lebanon stepover other than the Yammouneh Fault.

Many studies have noted that the Homs Basalt has an apparent left-lateral offset (Figure 4). The amount of offset was estimated as $\sim 20 \text{ km}$ by Quennell (1984); others have since quoted a range of smaller values. However, studies have argued in contrast that this part of the DSFZ ceased to be active in the latest Miocene or earliest Pliocene (e.g., Girdler 1990; Butler *et al.* 1997, 1998; Butler & Spencer 1999). As already noted, other studies (e.g., Brew *et al.* 2001) have argued instead that this part of the DSFZ did not become active until the Pliocene. These hypotheses are, of course, contradictory, and this point requires resolution.

Girdler (1990) argued that the northern DSFZ can be regarded as inactive because of an apparent lack of seismicity. He noted microearthquakes located west of the line of the DSFZ through Lebanon, and thus deduced that active slip continues northward from the Israel-Jordan border region on a hypothetical offshore fault zone. However, as has been previously noted (e.g., Yurtmen *et al.* 2002), no direct evidence for the existence of this offshore fault zone has ever been identified. The presence of microseismicity west of the main DSFZ strand in Lebanon can instead be readily explained as a result of the distributed crustal deformation occurring in this region due to its position along the Lebanon stepover (Westaway 1995a). Some faults within this zone may indeed have accommodated tens to hundreds of metres of

Quaternary slip, and as much as several kilometres of slip since the Miocene (such as the $\sim 9 \text{ km}$ left-lateral offset of the Litani River by the Roum Fault; Figure 2) (e.g., Butler *et al.* 1997). The absence of seismicity along the Yammouneh Fault and the northern DSFZ in recent decades does not mean that these structures are inactive: they have of course experienced many large historical earthquakes (e.g., Ben-Menahem 1981; Ambraseys & Barazangi 1989; Westaway 1994a).

Butler *et al.* (1997) argued that the northern DSFZ has not slipped since the latest Miocene/earliest Pliocene using field evidence from northern Lebanon (Figures 4 & 6). In northernmost Lebanon the DSFZ follows the valley of the Chadra River, which flows northward – west of the Akroum mountain range – into the Al-Bugeia lake basin on the Syrian border. In this vicinity, basalt is directly juxtaposed along the DSFZ on its western side. However, at the northern end of the Al-Bugeia Basin, basalt plunges beneath the alluvium in this basin: but whether any of it abuts the DSFZ beneath this basin is not known. Butler *et al.* (1997) also reported that the basalt west of the Chadra Valley is exposed for $\sim 200 \text{ m}$ thickness – its base being locally not exposed. They reported that the DSFZ can be locally well identified by a zone of fracturing several tens of metres wide, with $\sim 10\text{--}15 \text{ m}$ width of fault gouge – indicating intense cataclasis – directly abutting the eastern margin of the basalt (Figure 6). They also reported that this fault gouge is made entirely of limestone fragments, with no basaltic material being found within it. They thus concluded that this fault has not slipped since the basalt erupted, such that the sub-vertical contact between this basalt and the fault gouge is a dipping unconformity.

This interpretation by Butler *et al.* (1997) thus requires that the western margin of the fault gouge was an exposed sub-vertical face before the basalt erupted, which seems unlikely. The absence of basalt clasts in the fault gouge can anyway be explained in a number of ways. First, limestone overwhelmingly comprises the preponderant rock type in this region. In comparison, the volume of basalt is small. Second, it is evident that much of the Homs Basalt has experienced severe alteration, due to prolonged chemical weathering. Any loose clasts within the fault gouge, derived originally from this basalt, may thus have since disintegrated as a result of this process. Third, where intact, basalt is stronger than limestone. Thus, once the basalt was initially cut by left-lateral

faulting, subsequent slip would be expected to be concentrated within the limestone, not within the basalt, making it difficult for basalt clasts to enter the fault gouge.

The disposition of Homs Basalt flow units relative to the DSFZ can be observed at many localities in western Syria. Outside the linear valley that follows the DSFZ, flow units of the Homs Basalt are invariably subhorizontally bedded, reflecting the very gentle tilting away from the DSFZ of the land surfaces on which they were deposited (Figure 5). However, along the flanks of this valley, where these flow units are clearly exposed they can be observed to be dipping inward towards this valley: they are indeed often observed to be interbedded with sloping palaeosols or other slope deposits. This geometry is particularly clear along the eastern (Arabian) side of the Masyaf Fault around Alkollatia (Y in Figure 4), where a section through the sloping basalts and interbedded palaeosols has been exposed during construction of an irrigation canal, and on its western (African) side, south of Shmiyseh, just north of the Lebanon border (Z in Figure 4), where the basalt section has been exposed by quarrying. This is clear evidence that this linear valley already existed at the time of eruption of the Homs Basalt, which means that the DSFZ pre-dates this eruption. This evidence differs from what Butler *et al.* (1997) observed in northern Lebanon, where the basalt abutting the Chadra valley from the west is subhorizontally bedded (Figure 6). However, they did

note that the older basalt flow unit in this area is pillowed, indicating a sub-aqueous eruption, which implies the existence of a localised topographic depression at this time.

As already noted, estimating the amount of left-lateral slip since ~5 Ma from the disposition of the Homs Basalt is problematic. The fact that its linear valley existed before the basalt was erupted, such that many flows entered this linear valley from either side, means that one cannot simply correlate any individual flow from one side of this fault zone to the other [as for instance Yurtmen *et al.* (2002) have done across the Amanos Fault farther north]. Also, the fact that this linear valley already existed means that one cannot assume that equivalent relief existed at any locality on both sides of the fault at the time of basalt eruption. It is therefore not possible to derive any particular precise slip estimate from the Homs Basalt. A more pertinent issue is whether there is any evidence from the vicinity of the Homs Basalt to contradict the ~17–19 km of slip estimated since the end of basalt eruption at ~5 Ma, or the ~22–25 km estimated since its start at ~6.5 Ma. The answer is clearly no: for instance, restoring ~20 km of slip would juxtapose the thickest basalt west of the DSFZ, in northernmost Lebanon (around locality X in Figure 4) with the thickest basalt east of it in the area west of Shin in Syria (locality W in Figure 4). It will take a vast programme of fieldwork in this region to settle this point with any greater precision.

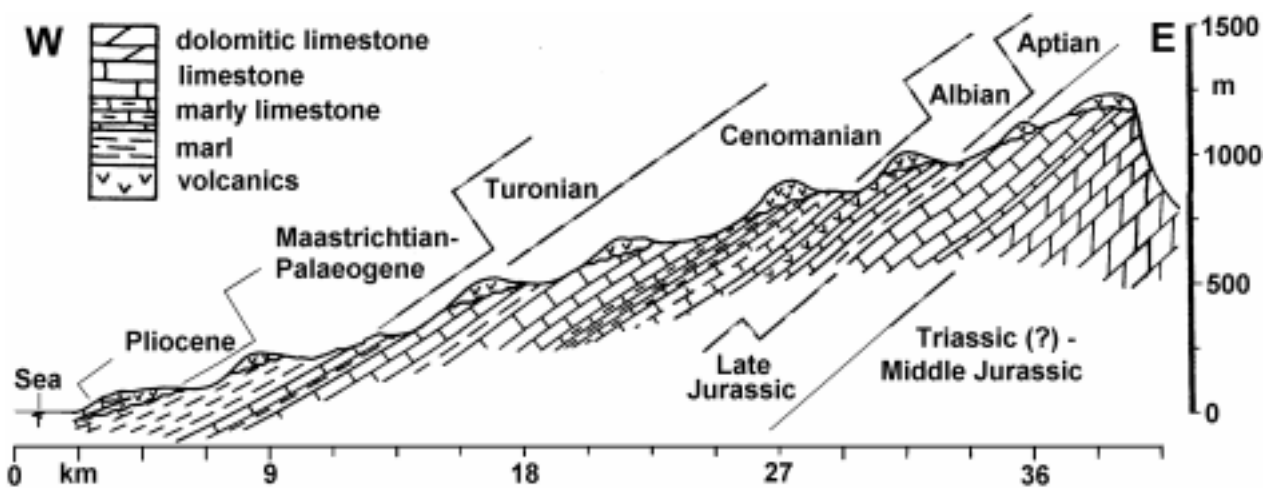


Figure 5. East-west cross-section located ~5 km north of Mashta (Figure 4), showing the disposition of Miocene basalt in relation to the Mesozoic sedimentary sequence (adapted from Mouty *et al.* 1992, figure 5).

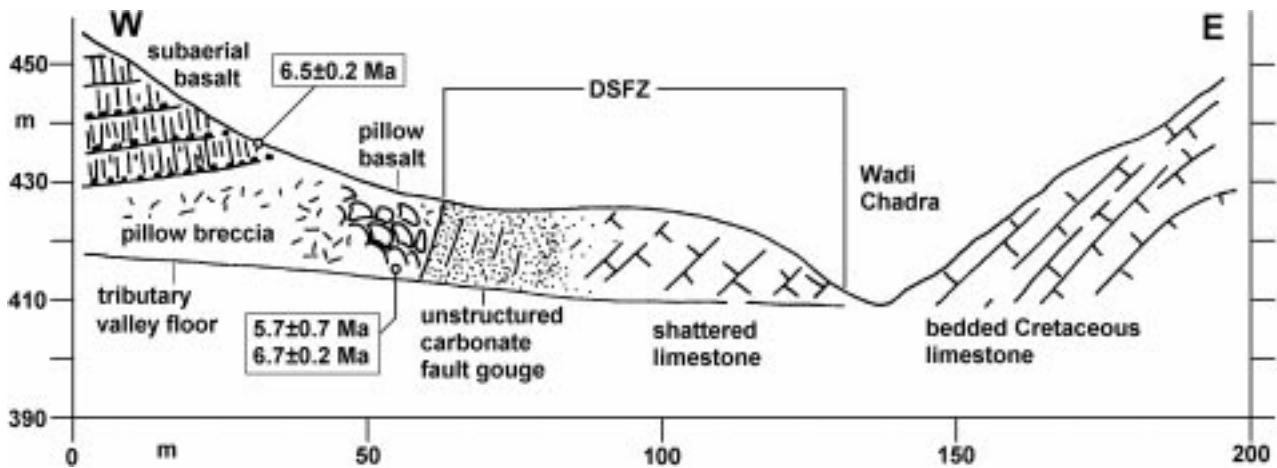


Figure 6. Cross-section across the DSFZ in northernmost Lebanon, adapted from Butler & Spencer (1999, figure 5) (see also Butler *et al.* 1997, 1998) showing the northern end of the active Yammouneh Fault in the Wadi Chadra Valley in northernmost Lebanon. See text for discussion.

The Ghab Basin in Northern Syria and Its Surroundings

The Ghab Basin is revealed by a Quaternary alluvial plain at ~100 m altitude, ~60 km long (N-S) and ~10 km wide, located on the northern DSFZ (Figures 2 & 3). Both its margins are bounded by left-lateral faults (Figures 2 & 3). The escarpment at its western margin, which forms the eastern flank of the Jabal Nusayriyah or Coastal Mountains, across which the land surface rises to up to 1562 m, is the more prominent of the two. Like farther south (Figures 4 & 5), the Mesozoic mainly carbonate sequence is exposed along both escarpments (Figure 3). Along both flanks these rocks are folded, pervasively broken up by minor faulting, and typically tilted away from the line of the DSFZ (e.g., Brew *et al.* 2001). The escarpment to the east is mostly in Cretaceous rocks, with some Tertiary cover still preserved on top (Figure 3). To the west, the more dramatic deformation has exposed much of the Jurassic sequence, with the Cretaceous preserved on top, but with almost all the former Tertiary cover eroded.

Most previous studies (e.g., Matar & Mascle 1993; Westaway 1994a; Brew *et al.* 2001) have regarded the Ghab Basin as a pull-apart basin located at a leftward step between transform fault segments of the DSFZ. It indeed gives the strong impression of the classic “rhomb” shape of a pull-apart basin (Figure 2), as many global studies of strike-slip faulting (and, most recently, Brew *et al.* 2001) have noted. This study will suggest a fundamentally

different interpretation, which is consistent with the proposed kinematics of the rest of the DSFZ: the Ghab Basin owes its existence to the local component of extension across a splay in the DSFZ, which is located within what is on a larger scale a transpressional stepover. The resulting interpretation thus resembles the overall geometry deduced by Westaway & Arger (1996) for the smaller Gölbaşı Basin on the EAFZ (Figure 1).

Satellite images (e.g., Muehlberger & Gordon 1987; Perinçek & Çemen 1990) and local mapping (e.g., Shatsky *et al.* 1963; Ponikarov *et al.* 1966) indicate that the DSFZ splays in the vicinity of the Ghab Basin (Figures 2 & 3). Its western strand, for which I suggest the name Nusayriyah Fault, follows the western margin of this basin, trending almost due N-S. Its eastern strand follows the eastern margin of the southern two-thirds of the basin (south of locality N in Figure 3), before heading off towards N10°E (Figure 2). I suggest the name Apamea Fault for the fault that bounds the eastern margin of the Ghab Basin and continues for ~20–25 km northward to a separate Quaternary depocentre: the ~25-km-long and up to ~5-km-wide Rouj Basin (the “Balou Trough” of Brew *et al.* 2001) (Figure 3). The proposed component of local extension that has created the Ghab Basin thus results from the component of northward divergence between these fault strands.

Farther north, the topography, geomorphology, geological mapping (e.g., Ponikarov *et al.* 1966), and satellite image interpretation (e.g., Muehlberger &

Gordon 1987; Perinçek & Çemen 1990) suggest that four significant distinct faults are present. One forms a northward end-on continuation of the Nusayriyah Fault along the western flank of the Orontes valley, before disappearing beneath the Holocene sediment of the Amik Basin across the Turkish border. I suggest the name Qanaya-Babatorun Fault for this structure, named after the largest villages along it (Figure 3). If the ~10 km apparent offset of the Early Pliocene marine sediment across it (I-J in Figure 3) represents a true left-lateral offset, this is evidently the most important active fault segment in this region. Seismic reflection profiling by Perinçek & Çemen (1990) reveals the subsurface continuation of this structure beneath the Amik Basin: it steps to the left and links end-on with the Amanos Fault that forms the western margin of the Karasu Valley farther north (e.g., Yurtmen *et al.* 2002). The other three faults become apparent north of the Rouj Basin, suggesting that – like the Ghab Basin – it marks a splay in the faulting (Figure 3). The easternmost of these, the Afrin Fault, continues NNE across northernmost Syria and appears to link end-on with other Late Cenozoic strike-slip faults in the Gaziantep area of southern Turkey (e.g., Coşkun & Coşkun 2000; Yurtmen & Westaway 2001b), notably the Kırkpınar Fault of Westaway & Arger (1996) (Figure 7). The Armanaz Fault continues northward, past the town of the same name, forming the eastern margin of an abrupt, ~700-m-high ridge formed of Eocene to Early Miocene marine sediment, then passing beneath the town of Harim and crossing the Turkish border. It can then be projected northward beneath the Holocene alluvium of the eastern part of the Amik Basin just west of Reyhanlı, before crossing back into Syria and linking end-on into the East Hatay Fault (Westaway 1994a; Yurtmen *et al.* 2002), which follows the line of this border northward for ~50 km (Figure 3). It then re-enters Turkey near Tahtaköprü, where the border turns east, and where it appears to be offset left-laterally by ~10 km (Eo-Co or E1-C1; Figure 3). The fault forming the western margin of the ridge west of Armanaz is here designated as the Salqın Fault. However, as it approaches the Turkish border it becomes indistinct, and it is unclear whether it simply dies out (as shown in Figure 3), whether it continues northward to the Amik Basin (e.g., Muehlberger & Gordon 1987), possibly passing into the leftward step in faulting that links into the Amanos Fault, or whether it bends towards the NNE (e.g., Perinçek & Çemen 1990), suggesting that it may merge with the

northward continuation of the Armanaz Fault somewhere beneath the Quaternary alluvium west of Reyhanlı. Further fieldwork in the immediate vicinity of the Turkish-Syrian border is needed to clarify this point. However, as Yurtmen *et al.* (2002) have noted, it has so far proved impossible to obtain permission for such fieldwork from the authorities in either country.

Subsequent fieldwork has shown that the tentative suggestion by Westaway & Arger (1996), that faulting steps to the right near Tahtaköprü from the East Hatay Fault to the Kırkpınar Fault along a localised transpressional stepover through the Kartal mountain range (Figure 2), is incorrect (Figure 7). The alternative view suggested previously, by satellite image interpretation (e.g., Muehlberger & Gordon 1987; Perinçek & Çemen 1990), is thus once again supported: that faulting continues NNE along the eastern margin of the Karasu Valley for another ~50 km to the vicinity of Sakçagöz. Satellite image studies (e.g., Muehlberger & Gordon 1987; Perinçek & Çemen 1990) and geological mapping (e.g., Terlemez *et al.* 1997; Yurtmen & Westaway 2001b) (Figure 3) indicate the presence of many discontinuous fault strands typically oriented SW-NE or SSW-NNE across a broad zone in this region. This structural trend originally developed in this region as a result of the latest Cretaceous ophiolite obduction (e.g., Tolun & Pamir 1975). In many cases, it is difficult to determine whether any given structure with this trend in this region simply dates from that time or has been reactivated. However, it is evident that some structures with this trend in this region have been reactivated in the Neogene (e.g., Terlemez *et al.* 1997; Coşkun & Coşkun 2000; Yurtmen & Westaway 2001b; Figure 7). The local situation thus appears to be similar to that reported farther south along the DSFZ (e.g., Lovelock 1984; Walley 1998), with some Late Cenozoic fault segments developing by reactivation of pre-existing lines of weakness. This evidence suggests that a substantial proportion of the left-lateral slip since the DSFZ became active may step to the right across the limestone uplands north of the Kartal Mountains, and then along the western margin of the uplands of the Gaziantep Plateau east of Narlı and Pazarçık, linking the East Hatay Fault to the Kırkpınar Fault and/or the EAFZ in the Gölbaşı area (Figure 2).

Gravity and seismic reflection prospecting indicate that the sedimentary fill in the Ghab Basin is up to ~1700

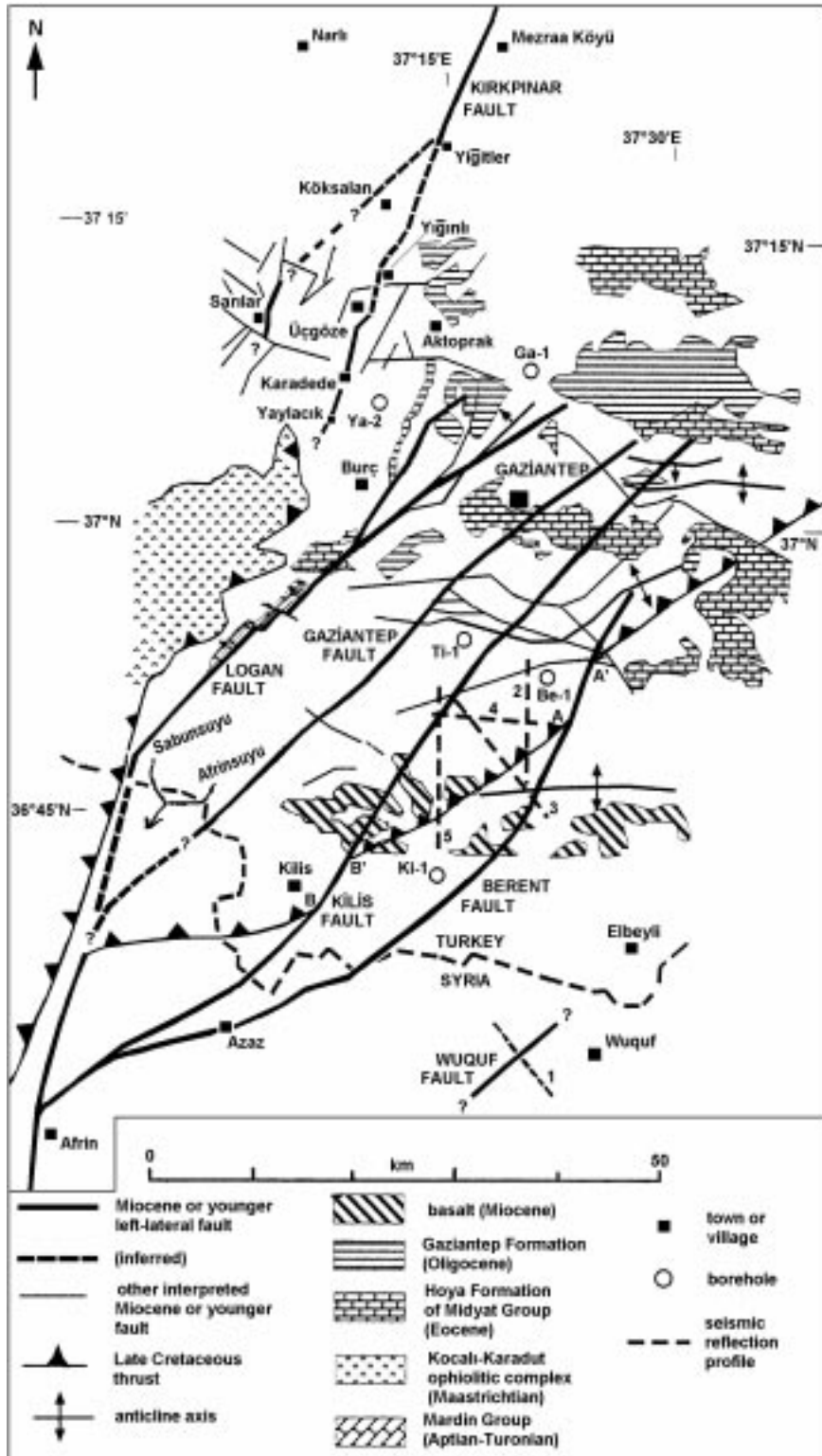


Figure 7. Map of the Turkey-Syria border region showing Late Cenozoic strike-slip faults in relation to thrust structures dating from the latest Cretaceous ophiolite obduction and selected Tertiary depocentres (adapted from Coşkun & Coşkun 2000, figures 2 & 9), also showing the Wuquf Fault from Chaimov *et al.* (1990) and the geometry of the Kirkpınar Fault and other information from Yurtmen & Westaway (2001b).

m thick (Brew *et al.* 2001). This fill consists almost entirely of Pliocene lacustrine sediment, the clastic component being derived from the Orontes River; in contrast, typically only a thin veneer of Quaternary sediment is present (e.g., Besançon & Sanlaville 1993; Domas 1994). Furthermore, drilling (into a limited number of localities on the basin flanks and one structural “high” in the basin interior) has revealed no Miocene fill between the Pliocene sequence and Eocene or Mesozoic bedrock (Brew *et al.* 2001). Interpretations of seismic reflection profiling (Brew *et al.* 2001) also suggest that there is no Miocene fill throughout the Ghab Basin, although this deduction is not confirmed elsewhere by drilling.

Brew *et al.* (2001) regarded this apparent absence of Miocene sediment as strong grounds for their interpretation that the northern DSFZ did not become active until the Pliocene. They also deduced that the outward tilting of the Mesozoic sequence, beyond both flanks of the DSFZ, developed before the DSFZ became active: this fault zone developing later along the N–S axis of this pre-existing anticline. However, it was suggested earlier from the disposition of the Homs Basalt that part of the equivalent tilting farther south has developed since the start of the Pliocene, implying that it has accompanied the Plio-Quaternary phase of slip on the DSFZ: presumably accommodating the required component of distributed shortening in its surroundings. It is suggested here that essentially the same geometry has existed across the Ghab Basin: the required component of distributed shortening and thickening, at a strain rate that increases towards the DSFZ from both sides, is causing the outward tilting observed on both sides.

A test of this interpretation is provided by the disposition of the Early Pliocene marine sediment, which provides an indication of the amount of uplift in each locality since deposition. This sediment is typically found at up to ~300 m altitude (e.g., Tolun & Erentöz 1962; Yurtmen *et al.* 2002), but crops out at up to ~600 m, instead, west of the Qanaya-Babatorun Fault: south of Babatorun in southernmost Turkey; and around Qanaya in Syria (Figure 3). Investigations of the Orontes terrace sequence (Bridgland *et al.* 2003) reveal – in contrast – no more than ~400 m of uplift since the latest Miocene/earliest Pliocene along reaches of this river (between Al Qusayr and Latamneh; Figure 2) that are several tens of kilometres east of the DSFZ. This uplift,

which does not vary measurably with position along this reach of the Orontes (Bridgland *et al.* 2003; see also e.g., Dodonov *et al.* 1993; Besançon & Sanlaville 1993), is interpreted as regional uplift: it is in localities that are east of the local tilting observed along the flanks of the DSFZ. One can thus presume that the ~600 m of uplift observed in the immediate vicinity of the DSFZ reflects this ~400 m of regional uplift plus an additional ~200 m local component of surface uplift caused by local crustal thickening to accommodate the distributed shortening along this transpressional segment of the DSFZ. It thus follows that local distributed crustal shortening and thickening have been significant in the immediate vicinity of the DSFZ during at least part of the time-scale since the Early Pliocene (contra Brew *et al.* 2001).

Furthermore, the existence of splays in the faulting (Figures 2 & 3) means that the deduction by Brew *et al.* (2001), that the Ghab Basin did not exist in the Miocene (which is itself equivocal due to the limited borehole control), does not mean that no strand of the northern DSFZ existed then. The relative motion between the African and Arabian plates in the Miocene could instead have been accommodated on the Apamea Fault and its in-line continuations to the north, which required no leftward step in the faulting. The geometry of left-lateral faulting could have changed in the Early Pliocene, with some (possibly, most) of the subsequent slip accommodated on the Nusayriyah and Qanaya-Babatorun faults instead (which did require a leftward step). It has been suggested that the geometry of the Arava segment of the DSFZ changed in the Early Pliocene, and it is suggested later that the geometry of the left-lateral strike-slip faulting farther north also changed at this time, when the EAFZ came into being. To suggest a change in the kinematics at a locality in between at an equivalent time is thus not unreasonable. Other explanations for the apparent lack of Miocene sediment in the Ghab Basin can also be envisaged: for instance, first, the present course of the middle and upper Orontes into the Ghab Basin developed in the earliest Pliocene (e.g., Bridgland *et al.* 2003). The absence of significant fluvial sedimentation in the Ghab Basin in the Miocene may thus reflect a lack of sediment input due to the absence of any major river flowing into this basin at the time. Second, throughgoing drainage between the Ghab and Rouj basins may have existed in the Miocene, before they became isolated by the local Pliocene volcanism (Figure 3). If the

Rouj Basin was at a lower level at the time, little or no deposition would be expected in the Ghab Basin.

During the Late Pliocene, the northern Ghab Basin was affected by basaltic volcanism (e.g., Besançon & Sanlaville 1993; Domas 1994) (Figure 3). Basalt flowed westward into this lake basin, ponding it near its northern outlet around the town of Jisr ash-Shugur (Figure 3). The subsequent surface uplift has led to the relatively easily eroded Miocene and Pliocene sediment north of this point along the Orontes valley becoming dramatically incised. However, the strength of this basalt “dam” allowed lacustrine sedimentation to continue for a time farther upstream (Domas 1994): the youngest lacustrine sediment in the Ghab Basin being biostratigraphically dated to Astian (i.e., latest Pliocene; ~2 Ma) age (Besançon & Sanlaville 1993). The subsequent development of this basin (involving minimal sedimentation or erosion) may simply relate to the slow progressive partial incision by the Orontes through the upper part of this basalt “dam”: it does not require another change in the regional kinematics.

It was earlier suggested that the total slip on the Amanos Fault is ~45–50 km from the offset of the southern margin of the Hatay ophiolite (F-G or F-H in Figure 3). Earlier discussion also suggests that the present geometry involves slip on the Amanos Fault stepping to the left, across the Amik Basin at its southern end, onto the Qanaya-Babatorun and Nusayriyah faults, with slip then again stepping to the right across the Ghab Basin. However, if the Ghab Basin did not exist beforehand, this geometry can only have existed since the Early Pliocene. The ~10 km of apparent slip since the Early Pliocene on the Qanaya-Babatorun Fault (I-J in Figure 3) could thus reflect the total slip on this structure. If so, the bulk of the ~45–50 km of slip on the Amanos Fault must have occurred in the Miocene, but continued south on another fault strand. It is thus possible that in the Miocene, the main southward continuation was the Salqin Fault, not the Qanaya-Babatorun Fault (Figure 2).

On the other hand, the lengths of other pull-apart basins and splay basins on the strike-slip faulting in the eastern Mediterranean region do roughly match the total slip on the adjoining faults. Examples are the Gölbaşı Basin on the EAFZ (Westaway & Arger 1996), the Hazar Basin on the EAFZ (see below), the Ovacık Basin on the Malatya-Ovacık Fault Zone (Westaway & Arger 2001),

and the Marmara Basin on the NAFZ (Westaway 1994a; Armijo *et al.* 1999). If this “rule of thumb” is applied to the faulting in northern Syria, the ~25 km length of the Rouj Basin would provide a rough indication of the combined slip on the Salqin and Armanaz faults. The substantial width of its “rhomb” shape means that the ~60 km length of the Ghab Basin will overestimate the slip on the Nusayriyah Fault: the ~45 km lengths of its N–S-trending margins provide an effective upper bound. Other slip estimates can be obtained by considering the geometry of the different splays in this faulting. Restoring 40 km of slip on the Nusayriyah Fault would juxtapose point N (Figure 3), where the Apamea Fault now bends NNE away from the Ghab Basin, against this basin’s southern end, thus “closing” the basin. This is thus an effective upper bound to the slip on the Nusayriyah Fault. Point P (Figure 3) indicates a best estimate of the point at which the Armanaz Fault splays from the Afrin Fault. The maximum feasible slip restoration would appear to place this point initially adjacent to the bend in the Apamea Fault at point N, ~25 km SSW, thus indicating the combined slip on the Salqin and Armanaz faults. The total slip on the Afrin Fault is not estimated by this reasoning. However, the relatively subdued relief (no more than ~200 m at most) across the escarpment along it between the Rouj Basin and the Ad Dana area on what is expected from the geometry to be transpressional stepover (Figure 3) suggests that it has probably not slipped as far as the other fault segments.

These upper bounds to the combined total of slip on the Nusayriyah, Salqin, and Armanaz faults of ~65 km roughly match the combined upper bounds of ~60 km on the Amanos (~50 km) and East Hatay (~10 km) faults. The partitioning of slip thus indicated suggests that significant slip (at least ~10 km) has indeed stepped leftward from the Amanos Fault to the Salqin Fault. However, ~40 km is far too much slip to have occurred on the Nusayriyah Fault to be compatible with the Pliocene age of the Ghab Basin suggested by Brew *et al.* (2001). It is thus evident that important issues concerning the timing of slip on individual fault segments in northern Syria, the detailed geometry of the basins along it (the respective contributions of splays versus pull-aparts), and the possibility of changes to the sense of slip remain to be fully resolved. Such investigation will require more thorough fieldwork in this sensitive region, beyond the scope of this study.

Faulting in the Karasu Valley

As already noted, the ~200-km-long Amanos Fault appears to form, after a leftward step across the Amik Basin, a northward continuation of the Qanaya-Babatorun Fault: bounding the western margin of the Karasu Valley and the eastern flank of the Amanos Mountains (Figures 2 & 3). As summarised by Yurtmen *et al.* (2002), the literature on this fault contains a great diversity of views as to its slip sense (whether mainly left-lateral or mainly normal faulting), slip rate (estimates range from a few tenths of 1 mm a⁻¹ to many millimetres per year), and overall role in the regional kinematics. To help resolve this contention, Yurtmen *et al.* (2002) undertook K-Ar dating of basalts that have flowed from the Amanos Mountains into the Karasu Valley and are offset left-laterally across the Amanos Fault by measured distances. Key sites investigated were at Hassa, Hacilar, and Küreci (locality A in Figure 3), and Karaçağıl, Ceylanlı, and Büyük Höyük (locality B in Figure 3). The results indicate that the strand of the Amanos Fault between Kırıkhan and Hassa (Figure 2) has a slip rate of ~1.0 to ~1.6 or ~1.7 mm a⁻¹. The interpretation of these results assumed, following Westaway (1994a), that the DSFZ is locally a transform fault zone slipping at ~7 mm a⁻¹. Yurtmen *et al.* (2002) thus concluded that the Amanos Fault takes up no more than ~20% of the AF-AR motion at present.

However, the revised AF-AR Euler vector, discussed earlier, predicts ~4.6 mm a⁻¹ of relative motion towards N32°W in the vicinity of Hassa (~36.7°N, ~36.5°E). As this is oriented at ~52° to the ~N20°E trend of the Amanos Fault, the maximum possible local rate of left-lateral slip can be estimated (using (1)) as ~4.6 mm a⁻¹ x cos(52°) and is ~2.8 mm a⁻¹. On this basis, it can be estimated that in this vicinity the Amanos Fault takes up at least ~40% (~1/~2.8) to ~60% (~1.7/2.8) of the AF-AR motion.

GPS (McClusky *et al.* 2000) now also allows the partitioning of slip across the various strands of the northern DSFZ to be investigated. Ground control point SAKZ (Sakçagöz) is located near the northern edge of the limestone uplands just east of the northernmost Karasu Valley. It is thus probably north of any fault segment running through these uplands linking the East Hatay Fault with the Kırkpınar Fault or the EAFZ near Gölbaşı (Figures 2 & 8a). Point GAZI (Gaziantep) is east of all known strands of the DSFZ in southern Turkey. The GAZI-SAKZ relative motion thus indicates the overall slip

rate across the Kırkpınar Fault and the subparallel fault zone east of Narlı and Pazarcık, which is expected to roughly equate to the combined slip across the Afrin and East Hatay faults farther south. This relative motion is determined (from McClusky *et al.* 2000) as 2.0±1.8 mm a⁻¹ northward and 1.3±1.9 mm a⁻¹ eastward, or ~2.4±2.6 mm a⁻¹ towards the ~NNE; it is thus not yet well resolved by GPS. In principle, one could add this ~2.4 mm a⁻¹ to the ~1.0–1.7 mm a⁻¹ slip rate on the Amanos Fault to get ~3.4–4.1 mm a⁻¹, which would more than cover the predicted ~2.8 mm a⁻¹ of NNE relative motion across the DSFZ in this vicinity. Some of this ~2.4 mm a⁻¹ of estimated relative motion could be occurring on the Kırkpınar Fault, or on other faults running west of it but east of SAKZ (shown schematically in Figures 2 & 8; see also Terlemez *et al.* 1997), which link to the EAFZ near Gölbaşı. However, some of the “missing” ~40–60% of AF-AR relative motion (not accounted for by the Amanos Fault) could instead be taken up on faults to the west of SAKZ: for instance, a previously unrecognised fault zone continuing northward from the East Hatay Fault, running west of Sakçagöz, and then NNE beneath the Aksu alluvial plain to the vicinity of Narlı. Yurtmen & Westaway (2001b) estimated that the Kırkpınar Fault (Figure 7) has slipped left-laterally by a total of ~10 km but found no geomorphological evidence of Quaternary slip along it: its slip may thus have been concentrated during the early phase of DSFZ slip, in the Miocene. This is one locality where future constraint on the kinematics is likely to be derived mainly from GPS.

North of Hassa, there are no Quaternary basalt flows crossing and offset by the Amanos Fault, which could constrain its slip rate – unlike farther south. Views have differed as to whether this part of the Amanos Fault is active at a significant slip rate (e.g., Şaroğlu *et al.* 1992) or not (e.g., Westaway & Arger 1996; Yurtmen *et al.* 2002), the latter view being supported by the more subdued relief across the fault. Many people (e.g., Şaroğlu *et al.* 1992) have argued that slip continues northeastward in the vicinity of Türkoğlu from the NNE-trending northern Amanos Fault onto the ENE-trending Gölbaşı-Türkoğlu Fault (Figure 2). Unfortunately, the junction (or intersection?) between these faults is hidden beneath the thick alluvium of the Aksu alluvial plain, and is thus not observable in the field. An argument against this possibility (by Westaway & Arger 1996) holds that such an abrupt ~45° bend in strike-slip faulting is not

feasible, as it would require major deformation in the fault's surroundings, which is not observed. However, that view was based on the assumption that both the Amanos Fault and the Gölbaşı-Türkoğlu Fault are transform faults. Since it is now clear that the Amanos Fault is NOT a transform fault, this kinematic objection is removed. It can indeed now be argued that the more subdued relief across the northern Amanos Fault may relate to a progressive reduction in the component of distributed shortening required to accommodate its left-lateral slip, as one passes from the southern Amanos Fault (which as previously noted can be regarded as a transpressive stepover on the DSFZ) to the Gölbaşı-Türkoğlu Fault (which can be regarded as taking up a component of the TR-AR relative motion; see below).

The East Anatolian Fault Zone

The left-lateral EAFZ links the northern end of the DSFZ, which previous discussion has established is in the Gölbaşı-Türkoğlu area, to the NAFZ. Westaway & Arger (1996, 2001) have suggested that for most of its length the EAFZ behaves as a transform fault zone between the Arabian and Eurasian plates. The main exceptions are at its rightward steps where it crosses the Neotethys suture near Çelikhan and farther northeast in the Gökdere Mountains near Bingöl (Figure 1). Furthermore, Westaway & Arger (2001) noted that at its intersection with the right-lateral NAFZ near Karlıova (the notional "triple junction" between the Turkish, Arabian, and Eurasian plates), distributed deformation is required in the surroundings to one or other fault. Westaway & Arger (2001) deduced that the most likely present-day geometry involves distributed EAFZ-parallel shortening and distributed NAFZ-parallel extension in the angle between the easternmost EAFZ and the projection of the NAFZ to the east of Karlıova (see their figure 14a). This geometry means that at points on the EAFZ near Karlıova, less slip will have occurred than on its transform-faulting segments farther SW. The frequently quoted measurement of 22 km of total slip just SW of Karlıova (e.g., Arpat & Şaroğlu 1972; Şaroğlu *et al.* 1992; Westaway 1994a) is thus expected to underestimate the total slip on the transform faulting segments of the EAFZ.

In the vicinity of the Hazar pull-apart basin, a total of up to ~35 km of left-lateral slip is evident on the EAFZ

(e.g., Westaway 1994a). In this vicinity, this fault zone has two en-echelon strands (Figure 1): the Hazar-Şiro Fault that enters the Hazar pull-apart from the SW, and the Çüngüş Fault farther SE. The ~5 km left-lateral offset of an ancient thrust fault near Hazar town (e.g., Yazgan 1983; Michard *et al.* 1984) suggests 5 km of total slip on the Çüngüş Fault. The ~30 km total length of the lowlands forming the Hazar pull-apart basin (of which 21 km is occupied by Lake Hazar) suggests the total slip on the Hazar-Şiro Fault. Farther SW, near Malatya, the gorge of the river Euphrates is offset left-laterally by 13 km where it crosses the Hazar-Şiro Fault. Many studies have thus quoted 13 km as its total slip. However, it now seems clear that the incision of this gorge post-dates the initiation of slip on this fault segment (e.g., Westaway & Arger 2001).

Farther SW, the main constraint on the overall EAFZ kinematics comes from the Westaway & Arger (1996) study of the Gölbaşı Basin, where the main EAFZ strand – the Göksu Fault – splays into the WSW-trending Gölbaşı-Türkoğlu Fault and the SSW-trending Kırkpınar Fault and its en-echelon counterparts (Figure 2). The left-lateral offset of an ophiolite body cut by the Gölbaşı-Türkoğlu Fault indicates that it has taken up 16 km of total slip. Westaway & Arger (1996) deduced a total of 33 km of slip across the Gölbaşı Basin from its geometry and from the left-lateral offset of a distinctive anticline axis used as a piercing point; thus estimating a total of 17 km of slip on the Kırkpınar Fault (and its SSW-trending counterparts). However, as Westaway & Arger (1996) noted, this measurement underestimates the total TR-AR relative motion due to neglecting the component of slip on the Sürgü Fault, which splays from the Göksu Fault farther northeast near Çelikhan (Figure 2). Near Kandil (Figure 2) the Ceyhan River flows parallel to the Sürgü Fault for ~8 km, before crossing it. However, detailed maps, such as by Perinçek & Kozlu (1983, figure 1), show the river ~2 km from the fault along this reach, suggesting that it is an instance of fortuitous alignment, not a true left-lateral offset. Farther east at Derbent, mapping by Perinçek & Kozlu (1983, figure 2) shows an ancient reverse fault, along which Palaeozoic rocks have been thrust eastward over Tertiary rocks, apparently offset left-laterally by ~4 km. None of the GPS points discussed by McClusky *et al.* (2000) provide useful constraint on the slip rate on the Sürgü Fault. Point KDRL is located just east of the Yakapınar-Göksun Fault, its

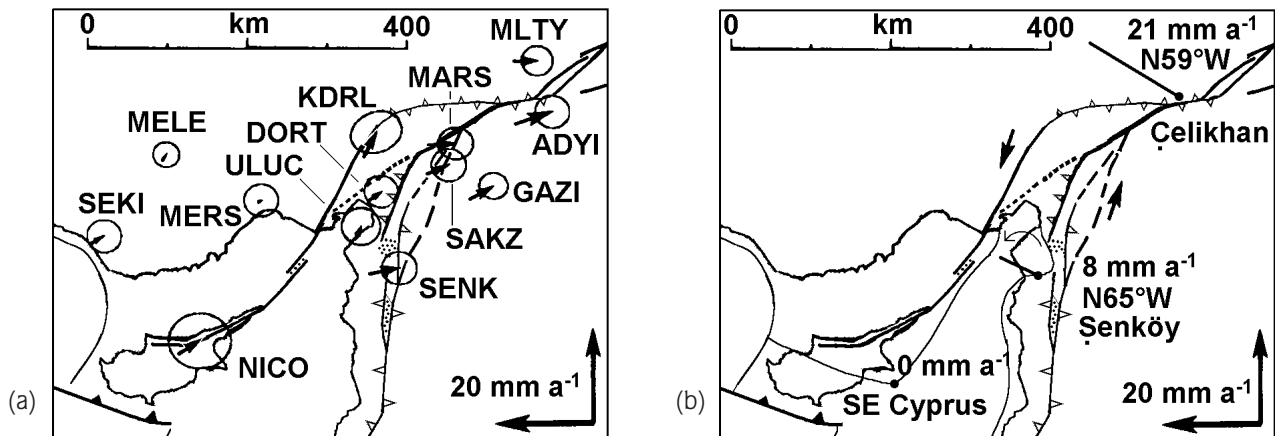


Figure 8. Maps of the “triple junction” region between the Turkish, African, and Arabian plates. (a) Positions and motions relative to the Turkish plate of GPS points in relation to major faults (adapted from McClusky *et al.* 2000, figure 7). (b) Kinematic model for this region, showing location of relatively strong continental crust (shaded), the area of anticlockwise rotation (and/or distributed left-lateral simple shear) affecting a strong block “trapped” between the Arabian and Turkish plates. Thick lines indicate estimated rates and senses of mantle lithosphere flow relative to the stable interior of the African plate. See text for discussion.

southwestward end-on continuation (Figures 2 & 8b). However, no other point is located close enough to this fault on its west side to provide any useful constraint. Future densification and repeat GPS observation in this locality could thus provide useful constraint on its slip rate.

Westaway (1994a) deduced from TR-AR-EU velocity vector triangle closure that the EAFZ has a slip rate of $\sim 13 \text{ mm a}^{-1}$. However, his $\sim N10^\circ W$ sense of AF-AR relative motion in this region was based on the assumption that the DSFZ in Syria is a transform fault zone, and is thus substantially in error. Revised vector triangles can be determined instead using the McClusky *et al.* (2000) GPS solutions for the TR-EU and TR-AR Euler vectors ($1.2^\circ \text{ Ma}^{-1}$ about $30.7^\circ N, 32.6^\circ E$; and $0.5^\circ \text{ Ma}^{-1}$ about $25.6^\circ N, 19.7^\circ E$, respectively). These solutions predict an EAFZ slip rate of $\sim 8 \text{ mm a}^{-1}$ towards an azimuth that rotates progressively concave-southward from $S65^\circ W$ at Hazar to $S48^\circ W$ at Gölbaşı (Figures 1 & 9). This reduction in slip rate requires an increase in the estimated age of this fault zone from $\sim 3 \text{ Ma}$ (Westaway & Arger 1996, 2001) to $\sim 4 \text{ Ma}$. Neglecting for the time being the contribution from the Sürgü Fault, the slip rates on the Gölbaşı-Türkoğlu Fault and Kırkpınar fault system can be estimated as ~ 4.0 and $\sim 4.3 \text{ mm a}^{-1}$ ($\sim 16 \text{ km/4 Ma}$ and $\sim 17 \text{ km/4 Ma}$), respectively. For comparison, SW of Gölbaşı, all three of the tributary gorges of the Aksu River that cross the Gölbaşı-Türkoğlu Fault are offset left-laterally by $\sim 3.5\text{--}4 \text{ km}$. Westaway & Arger (1996)

suggested that the entrenchment of these river gorges, which led to the rivers becoming “locked” in their courses and so progressively offset, began around OIS 22 at $\sim 0.87 \text{ Ma}$. The resulting slip rate estimate is thus ~ 4.0 to $\sim 4.6 \text{ mm a}^{-1}$, in better agreement with the EAFZ slip rate derived from the McClusky *et al.* (2000) GPS results than the older Westaway (1994a) kinematic model.

It was previously suggested that the bulk of slip on the Gölbaşı-Türkoğlu Fault may continue southward on the Amanos Fault (Figure 2), after a $\sim 45^\circ$ bend at Türkoğlu: the Gölbaşı-Türkoğlu Fault being a transform fault segment and the Amanos Fault surrounded by distributed deformation. If this deformation is concentrated west of the Amanos Fault, then the upper bound to the slip rate on the Amanos Fault can be estimated as $\sim 4 \text{ mm a}^{-1} \times \cos(45^\circ)$ or $\sim 2.8 \text{ mm a}^{-1}$, similar to the value estimated earlier from the kinematics of the DSFZ and consistent with the range of slip rates determined observationally by Yurtmen *et al.* (2002). The $\sim 4.3 \text{ mm a}^{-1}$ estimated slip rate on the Kırkpınar fault system near Gölbaşı exceeds the estimated $\sim 2 \text{ mm a}^{-1}$ slip rate on its southward continuation between the SAKZ and GAZI GPS points (Figure 8a). This discrepancy requires a component of Kırkpınar-Fault-parallel distributed deformation: either distributed NNE–SSW shortening on its west side or distributed NNE–SSW extension on its eastern side. The former alternative seems the more likely; this being another issue that GPS can potentially address in the future.

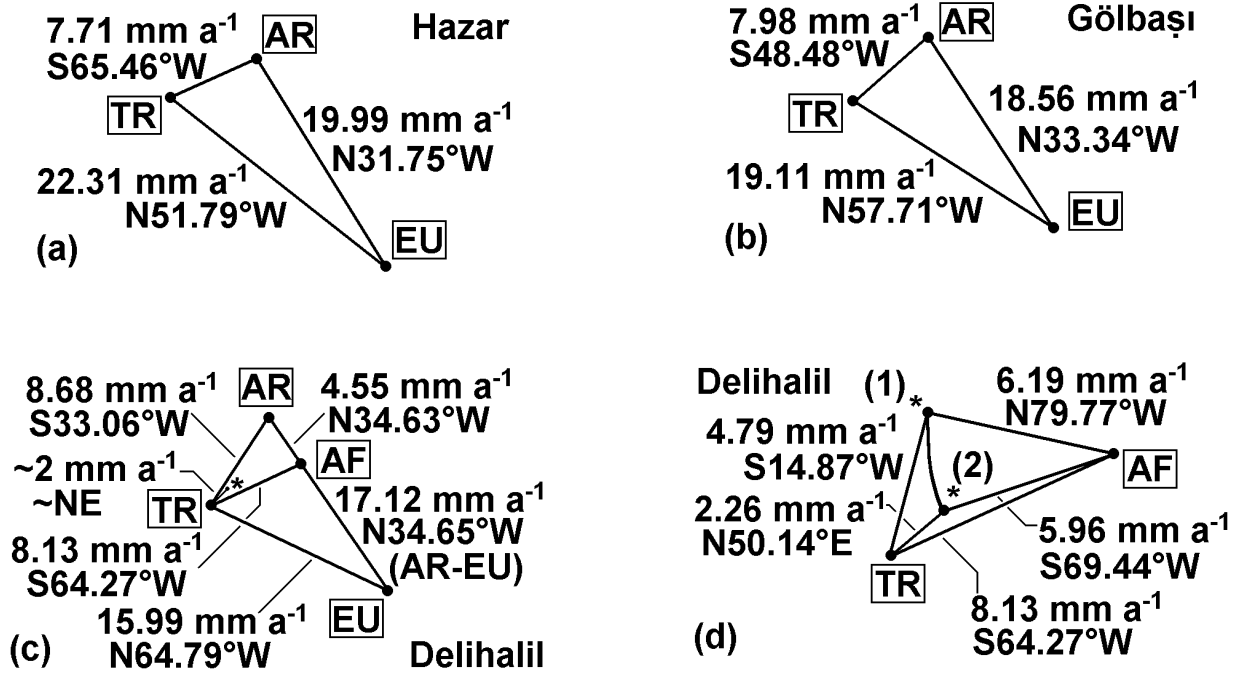


Figure 9. Velocity vector polygons. (a) at Lake Hazar on the EAFZ (38.5°N, 39.5°E); (b) at Gölbaşı on the EAFZ (37.8°N, 37.7°E); (c) at Delihalil within the TR-AR plate boundary zone (37.0°N, 36.0°E). Vector * indicates the motion of GPS points ULUC and DORT. (d) Enlargement of the key part of (c). The meaning of vectors (1) and (2) is discussed in the text.

NW of the EAFZ is a separate left-lateral fault system, the Malatya-Ovacık Fault Zone (MOFZ) (Figure 1). Westaway & Arger (1996, 2001) suggested that this formed the AR-TR plate boundary when the Turkish plate first came into being with the initiation of slip on the NAFZ. At this time, the eastern end of the NAFZ was at its intersection with the MOFZ near Erzincan, creating a geometry that had some similarity with the modern intersection at Karlova (Westaway & Arger 2001). Westaway & Arger (2001) estimated that 29 km of slip occurred on the transform-faulting parts of the MOFZ while it was active. Using the $\sim 13 \text{ mm a}^{-1}$ EAFZ slip rate from Westaway (1994a), they estimated that the EAFZ became active at $\sim 3 \text{ Ma}$ and that the MOFZ was active during $\sim 5\text{--}3 \text{ Ma}$. Adjusting the EAFZ slip rate to $\sim 8 \text{ mm a}^{-1}$ suggests instead that the EAFZ became active at $\sim 4 \text{ Ma}$ and that the MOFZ became active at $\sim 7\text{--}8 \text{ Ma}$ and was active until $\sim 4 \text{ Ma}$. This pushes the initiation of the NAFZ back in time from the Early Pliocene ($\sim 5 \text{ Ma}$) age preferred by Westaway (1994a) and other studies to around the Tortonian–Messinian boundary in the Late Miocene.

The Turkey-Africa Plate Boundary

Offshore of southern Turkey, the TR-AF boundary is localised along the Misis-Kyrenia Fault Zone (e.g., Westaway & Arger 1996) (Figures 2 & 10). Possible alternative locations farther east, which have been suggested in the literature, do not stand up to careful scrutiny. This point has recently been discussed at length by Yurtmen *et al.* (2002) and is not repeated here. Once onshore, this boundary has been interpreted (e.g., Westaway & Arger 1996) as splaying into two left-lateral fault zones: the NE-trending Yakapınar-Göksun Fault, which links through to the Sürgü Fault and was the site of the June 1998 Ceyhan earthquake; and the ENE-trending Karataş-Osmaniye Fault, which links end-on to the Düziçi Fault in the Amanos Mountains (Figure 2). Westaway & Arger (1996) suggested that the Karataş-Osmaniye Fault is the more important of the two, with a slip rate of $\sim 5 \text{ mm a}^{-1}$. For much of its length, the line of the Karataş-Osmaniye Fault is obvious in the field: it follows an escarpment up to $\sim 200 \text{ m}$ high indicating a small component of relative upthrow of its NW side in addition to the predominant left-lateral slip. The significance of this escarpment was first recognised by

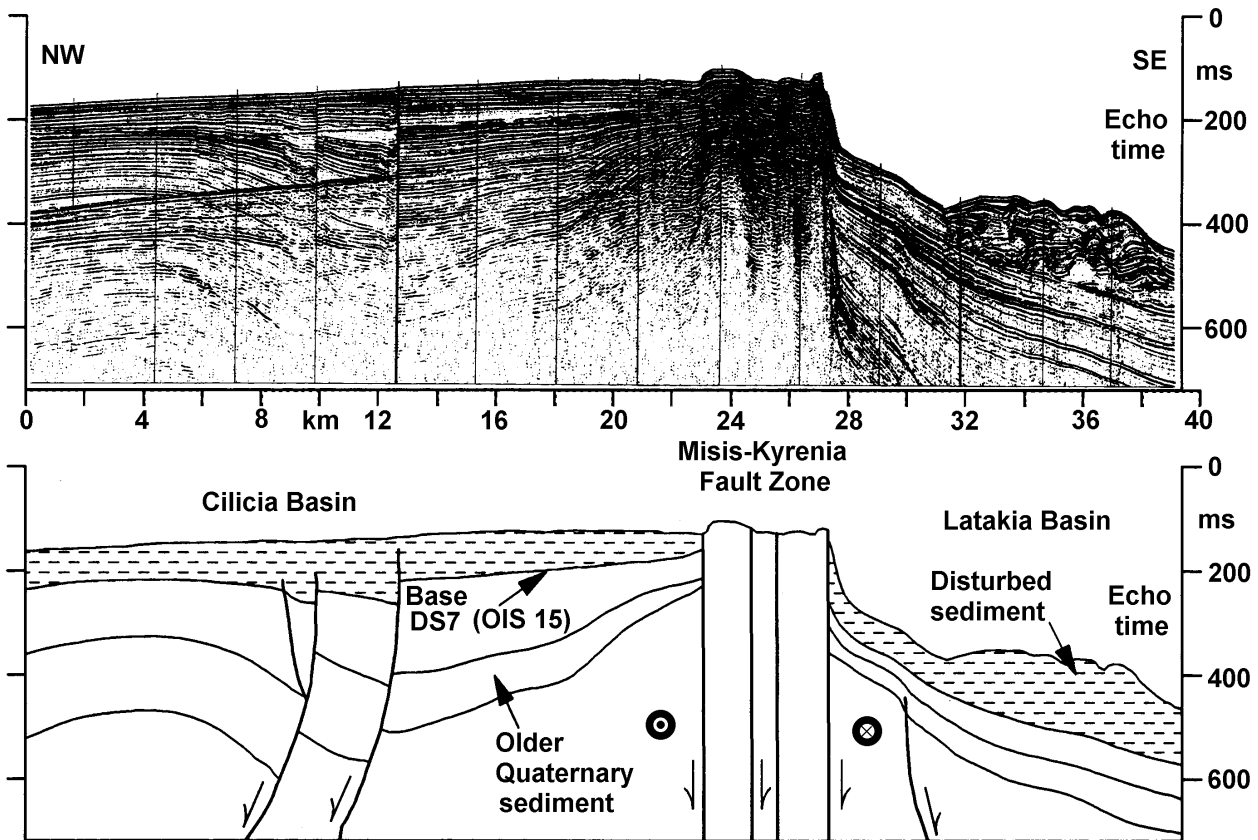


Figure 10. Seismic reflection record section and interpretation of a profile crossing the Misis-Kyrenia Fault Zone between Karataş and the Kyrenia Range on Cyprus (adapted from Aksu *et al.* 1992a, b, figure 8). Excluding effects of halokinesis, this is the clearest evidence of active crustal deformation offshore of the Levant coastline, and indicates where the most important offshore active fault zone in this region is located.

McKenzie (1976) using satellite imagery. However, near Osmaniye the line of the Karataş-Osmaniye Fault passes through the Ceyhan-Osmaniye volcanic field, of Quaternary age (e.g., Yurtmen *et al.* 2000; Arger *et al.* 2000; Yurtmen & Westaway 2001a): basalts from volcanic necks such as Toprakkale and Delihalil being found on both sides of this line. Westaway & Arger (1996) thought they had identified the line of the Karataş-Osmaniye Fault along an abrupt scarp edge to the Toprakkale Basalt, trending WSW away from this neck. However, this scarp has since been excavated during construction of an irrigation canal, revealing a section through it that establishes it as a river terrace scarp and not a fault scarp (Yurtmen & Westaway 2001a). Subsequent fieldwork here and farther SW around Delihalil (Yurtmen & Westaway 2001a) indeed reveals no evidence of any significant left-lateral offset along this fault line since the youngest basalt – dated to ~0.4 Ma

(Arger *et al.* 2000) – was erupted. It thus now seems clear that the Karataş-Osmaniye Fault is not active at present (contra Westaway & Arger 1996), although it clearly was an important left-lateral fault at an earlier stage.

Evidence in support of this point of view is also provided by the GPS data (McClusky *et al.* 2000), which report motions of three points situated between the DSFZ and the Karataş-Osmaniye Fault: SENK (Şenköy), ULUC (Uluçınar), and DORT (Dört Yol) (Figure 8a). As McClusky *et al.* (2000) noted, SENK is moving roughly as expected for a point within the African plate, but ULUC and DORT, farther northwest, are moving in a sense much closer to what is expected for points within the Turkish plate. Their motion is indeed roughly ~2 mm a⁻¹ towards the northeast relative to the interior of the Turkish plate, rather than the ~8 mm a⁻¹ towards ENE that is expected from the relative motions between these

plates. These GPS results have two main implications. First, there is significant relative motion between SENK and ULUC and DORT, which must involve distributed deformation as no major fault is present. Second, the overall left-lateral slip rate across the Karataş-Osmaniye and Yakapınar-Göksun faults is $\sim 2 \text{ mm a}^{-1}$. Since the slip rate on the former is now assumed to be zero, the slip rate on the latter can thus be estimated as $\sim 2 \text{ mm a}^{-1}$. This interpretation is also consistent with the motion of the GPS point KDRL (Kadirli), located between the Karataş-Osmaniye and Yakapınar-Göksun faults, which has negligible motion relative to ULUC and DORT.

This estimated slip rate of $\sim 2 \text{ mm a}^{-1}$ on the Yakapınar-Göksun Fault exceeds the $\sim 1 \text{ mm a}^{-1}$ slip rate on its continuation, the Sürgü Fault, estimated from its $\sim 4 \text{ km}$ of apparent slip since $\sim 4 \text{ Ma}$. This difference is consistent with the interpretation, suggested in Figure 1, that the Sürgü Fault can be regarded as a transpressional stepover from the Yakapınar-Göksun Fault, with a $\sim 65^\circ$ difference in strike. If so, the upper bound to the slip rate on the Sürgü Fault can be estimated (using (1)) as $\sim 2 \text{ mm a}^{-1} \times \cos(65^\circ)$ or $\sim 0.8 \text{ mm a}^{-1}$, roughly consistent with the local evidence.

Relative to SENK, ULUC is moving northward at $1.1 \pm 2.1 \text{ mm a}^{-1}$ and westward at $6.1 \pm 2.3 \text{ mm a}^{-1}$; DORT is moving relative to SENK at $0.7 \pm 2.0 \text{ mm a}^{-1}$ northward and $5.7 \pm 2.1 \text{ mm a}^{-1}$ westward (McClusky *et al.* 2000), this relative motion of ULUC (1) being illustrated in Figures 9c and d. Figure 9d also shows an alternative ULUC-SENK relative velocity vector (2), which is consistent (within error bounds) with the observed motion and also consistent with $\sim 2 \text{ mm a}^{-1}$ of slip on the Yakapınar-Göksun Fault. It results from assuming that the line joining ULUC and SENK is rotating anticlockwise around a vertical axis at 7° Myr^{-1} . Such a rotation could result either from anticlockwise rigid-body rotation of the block containing these points or from a component of distributed left-lateral simple shear across the zone containing the DSFZ and Yakapınar-Göksun Fault. A model that can account for this sense of deformation is proposed below.

There is, of course, no guarantee that the Yakapınar-Göksun Fault became active at the same time as the other faults forming the EAFZ. Below it is suggested that this fault came into being when pre-existing slip on the Karataş-Osmaniye and Düziçi faults became no longer mechanically feasible due to a local concentration in

normal stress resulting from convergence between high-strength crust in the İskenderun Gulf area and the normal crust of the Turkish plate interior. If this had not occurred, the TR-AF relative motion could still be accommodated on the Karataş-Osmaniye and Düziçi faults, at a rate of $\sim 8 \text{ mm a}^{-1}$ (Figure 9c). Westaway & Arger (1996) suggested that the Karataş-Osmaniye and Düziçi faults became active at the same time as the MOFZ, and may possibly have been linked to it. Using structural evidence in the Amanos Mountains, they estimated the total slip on the Düziçi Fault as $\sim 28 \text{ km}$, implying that it was active for $\sim 28 \text{ km} / 8 \text{ mm a}^{-1}$ or $\sim 3.5 \text{ Ma}$. It thus appears to have been active for longer than the MOFZ was (given earlier calculations), suggesting that for some time (maybe $\sim 0.5 \text{ Ma}$ during the Early Pliocene) the EAFZ already existed and linked through end-on into the Karataş-Osmaniye and Düziçi faults, the Yakapınar-Göksun Fault having not yet become active. Future investigations, for instance, investigating any possible change in the style of sedimentation in İskenderun Gulf, may better constrain the timing of the ending of slip on the Karataş-Osmaniye Fault, but are beyond the scope of this study.

The North Anatolian Fault Zone

The North Anatolian Fault Zone is a $\sim 1500\text{-km}$ -long right-lateral fault zone linking the Karlıova triple junction and the Aegean Sea (Figure 1), thus forming the boundary between the Turkish and Eurasian plates. Its concave-southward geometry allows the Turkish plate to rotate anticlockwise relative to Eurasia with minimal internal deformation (e.g., Westaway 1994a; McClusky *et al.* 2000). As already noted, it appears to have experienced two phases of slip: the first, conjugate to the MOFZ, when the NAFZ terminated in the east at Erzincan; and the second, which continues, conjugate to the EAFZ (Westaway & Arger 1996, 2001; Arger *et al.* 2000).

There is now close agreement between Euler pole fits to the NAFZ from geological evidence (e.g., Westaway 1994a) and GPS data (e.g., McClusky *et al.* 2000). The main difference between these solutions is that the GPS predicts somewhat higher NAFZ slip rates, $24 \pm 1 \text{ mm a}^{-1}$ against $17 \pm 1 \text{ mm a}^{-1}$. Westaway's (1994a) $\sim 17 \text{ mm a}^{-1}$ estimate was based on time-averaging the estimated $\sim 85 \text{ km}$ of slip since $\sim 5 \text{ Ma}$: it would decrease to $\sim 12 \text{ mm a}^{-1}$ if the revised $\sim 7 \text{ Ma}$ age of the NAFZ (suggested

earlier) were adopted instead. One possible explanation for these discrepancies is that the NAFZ slip rate has increased over time since it first formed. Another is that for most of the length of the NAFZ, Westaway's (1994a) slip restoration only covers its main strand, whereas the GPS measures the relative motion across all strands. Another is that the overall geometry of the NAFZ changed at the start of the present slip phase, estimated above at ~4 Ma, and the ~85 km slip estimate relates to the present slip phase, indicating a time-averaged rate of ~85 km/~4 Ma or ~21 mm a⁻¹. Another is that there is a component of NAFZ-parallel distributed simple shear close to this fault zone, in addition to its localised slip, which is picked up by the GPS not by the slip restoration. Resolution of this point is beyond the scope of this study (but see also below).

Important new evidence relating to the timing of initiation of the NAFZ has been provided by studies, by Tüysüz *et al.* (1998) and Armijo *et al.* (1999, 2000), of the faulting in the area between the Sea of Marmara and Saros Gulf in the NE Aegean Sea (Figure 1). Although some details of timing and interpretation differ between these papers, and have indeed been disputed (Yalırak *et al.* 2000), it is evident that throughgoing right-lateral faulting in this area did not begin until the Early Pliocene. The NAFZ strand in this vicinity has subsequently slipped right-laterally by ~70 km, as is revealed by the offset between axes of major truncated anticlines in the Ganos and Gelibolu areas (Figure 1) (Armijo *et al.* 1999, 2000). According to Armijo *et al.* (1999, 2000), these major anticlines developed during an abrupt phase of folding concentrated in the Messinian stage (~7–5 Ma), which affected the whole earlier Miocene sedimentary succession. Tüysüz *et al.* (1998) suggested that this folding was associated with the earliest phase of slip on the NAFZ, which involved reactivation by right-lateral slip of an older structure (the suture of the intra-Pontide ocean). However, because this structure is oriented roughly NE–SW, at ~20° to the NAFZ slip sense, significant distributed shortening was required in its surroundings (see Westaway 1995a) in order for slip to occur on it. However, Tüysüz *et al.* (1998) considered the age of this folding to be Early Pliocene, not Messinian. Assigning these events a definitive age depends on dating the clastic sediment shed by alluvial fans as a result of erosion of these actively-folding anticlines, which is known as the Conkbayırı Formation. These sediments are

not well dated: Tüysüz *et al.* (1998) summarised some limited evidence in support of a Pliocene age; but Armijo *et al.* (1999) implied a Messinian age for much of their succession (while admitting that this deposition probably also continued into the Pliocene). Armijo *et al.* (1999) indeed tentatively placed them in the stratigraphic sequence above the biostratigraphically dated early Late Miocene fluvio-lacustrine and marine Kirazlı Formation and partly below and partly interfingering with the marine sediments of the Alçitepe Formation that they took to represent the post-Messinian transgression. An arid climate, favouring alluvial fan deposition, is anyway to be expected in land areas flanking the Mediterranean basin during its Messinian regression.

Many studies (e.g., Barka & Kadinsky-Cade 1988; Westaway 1994a) have previously argued for Early Pliocene (~5 Ma) initiation of the NAFZ. However, a major difficulty with this view is that no known reason exists for why such a major structure should have developed at this time. As already noted, an adjustment in its age to ~7 Ma (Early Messinian) now appears necessary to account for the observed displacements on strike-slip faults in eastern Turkey, given the reduced slip rates favoured by the present new kinematic model. Including the early strongly-transpressional phase in the Saros-Marmara region, an Early Messinian age also appears evident for the NAFZ on the basis of this local evidence. A model is indeed suggested later that can account for the initiation of this fault zone in response to changes to the regional state of stress accompanying the dramatic fall in sea level that occurred during the Messinian regression of the Mediterranean Sea.

Regional Kinematic Models

Previous attempts at devising regional kinematic models for Turkey (e.g., Westaway 1994a; McClusky *et al.* 2000) have not been concerned with lithosphere rheology, just with the kinematic consistency between different localities. Many studies (e.g., Westaway 1994b, c, 1996, 1998, 1999a, b, 2001, 2002b, c, d, e; Mitchell & Westaway 1999; Arger *et al.* 2000; Westaway *et al.* 2002, 2003; Bridgland *et al.* 2003) have established that flow in the lower crust is essential to explain many aspects of the geological record. It thus now seems reasonable to incorporate this aspect of continental lithosphere rheology, and its implication that motions in

the brittle upper crust and mantle lithosphere can be decoupled, into kinematic models for Turkey. Flow in this weak lower-crustal layer seems necessary to explain the Late Cenozoic histories of surface uplift of different parts of Turkey (e.g., Westaway 1994b; Arger *et al.* 2000; Westaway *et al.* 2003). A weak lower-crustal layer can be expected from the high observed heat flow throughout western and central Turkey (e.g., İlkışık 1995; İlkışık *et al.* 1997; Pfister *et al.* 1998), which appears to result from the relatively thin mantle lithosphere caused by the relatively late (latest Precambrian) consolidation of the lithosphere of Turkey in the Pan-African orogeny (e.g., Arger *et al.* 2000). Of course, some localities – where the continental crust is thin (as offshore of the Levant coastline, indicated by the deep bathymetry: e.g., Vidal *et al.* 2000), or abnormally strong (e.g., where major ophiolite bodies are present) may lack the weak lower-crustal layer that is typical elsewhere – in which case the brittle layer and mantle lithosphere will locally be moving in the same sense and at the same rate.

Decoupling between upper crust and mantle lithosphere seems *a priori* necessary to explain the study region. The close spacing of individual faults in relation to the flexural wavelength of the mantle lithosphere means that, at best, the mantle lithosphere moves at a rate that approximates a spatial average of the motions in the overlying brittle upper crust (e.g., Westaway 2002b). No mantle lithosphere counterpart to the DSFZ, EAFZ, or NAFZ, let alone any of the smaller fault zones in the study region, has ever been reported using any type of evidence. Nor is there any evidence of mantle lithosphere downwelling beneath this region, other than the obvious subduction of the African plate beneath the southern margin of the Turkish plate. However, it is clear that the existence of oceanic spreading in the Red Sea requires the mantle lithosphere beneath Arabia to be moving laterally away from that beneath the African plate – but where to?

The GPS solutions (e.g., McClusky *et al.* 2000) indicate that, overall, the relative motions in the study region involve anticlockwise rotation of the upper crust forming the Turkish plate relative to Eurasia. It is presumed that at present the motion, relative to the African plate, of the mantle lithosphere beneath Arabia is accommodated by its motion in the same sense. There is thus no requirement for a localised “fault” in the mantle lithosphere beneath the NAFZ: just a zone with a lateral velocity gradient, with a southward increase in westward

velocity. In such a picture, shear tractions transmitted across the lower-crustal layer from the moving mantle lithosphere to the moving upper crust force the westward motion of the Turkish plate relative to Eurasia. This relative motion is in turn resisted by frictional tractions applied to the northern edge of this plate along the NAFZ. The cyclic release of such stresses, in the NAFZ earthquake cycle, permits the relative crustal motions that are observed. McClusky *et al.* (2000) suggested that the fact that the Turkish plate behaves as a rigid body implies that its lithosphere is strong. This new picture suggests a totally different explanation for this rigid-body behaviour: the brittle upper crust of the Turkish “plate” is quite weak, but it does not deform internally because a geometry of relative motions has developed in which it is able to move with negligible internal deformation in response to the forces acting on its base and edges.

Supporting evidence for this picture comes from the well-known clear mismatch between Euler vectors for the AF-AR relative motion determined from the DSFZ (e.g., Klinger *et al.* 2000) and from the oceanic spreading in the Red Sea (e.g., Chu & Gordon 1998). The former indicates motions of blocks of the brittle upper crust, the latter indicates motions of the mantle lithosphere; the fact that these motions are different requires the brittle upper crust and mantle lithosphere to be decoupled.

The mantle lithosphere flow beneath the vicinity of the NAFZ is thus assumed to involve a substantial velocity gradient perpendicular to the NAFZ. Unlike this, the mantle lithosphere flow that accommodates the difference in motions between the mantle lithosphere beneath the African plate and that beneath the Arabian plate is assumed to involve velocity gradients that are strongly oblique to the DSFZ. The reason for this is to enable this flow to “dovetail” smoothly into the westward mantle lithosphere flow beneath the Turkish plate, with no discontinuity in mantle lithosphere velocity across the EAFZ. It is thus inferred that much of this velocity gradient zone in the mantle lithosphere is located beneath the “promontory” of the African plate to the east of Cyprus. The component of northwestward velocity in the mantle lithosphere is thus inferred to increase from zero relative to the stable interior of the African plate at the eastern end of the Cyprus subduction zone to a value of $\sim 25 \text{ mm a}^{-1}$ relative to Eurasia at the mid-point of the EAFZ to roughly match the local average of upper crustal velocities (observed by GPS; McClusky *et al.* 2000) on the Turkish and Arabian sides of this fault zone.

Estimates, at representative points, of the velocity of the mantle lithosphere relative to the stable interior of the African plate are shown in Figure 11. The value of $\sim 21 \text{ mm a}^{-1}$ towards $\text{N}59^\circ\text{W}$ for the mantle lithosphere beneath the EAFZ at Çelikhan is obtained by subtracting the local estimate of $\sim 25 \text{ mm a}^{-1}$ towards the NW relative to Eurasia from the $\sim 7 \text{ mm a}^{-1}$ northward velocity of stable Africa (e.g., Westaway 1990) relative to Eurasia. The value for Şenköy, $\sim 8 \text{ mm a}^{-1}$ towards $\text{N}65^\circ\text{W}$, is based on the view that because this site is within the main body of Hatay ophiolite (Figure 3) the upper crust is likely to be coupled to the underlying mantle lithosphere. The local velocity of the upper crust (and mantle lithosphere) of Africa relative to Eurasia, of $\sim 12.6 \text{ mm a}^{-1}$ towards $\text{N}35^\circ\text{W}$ (estimated in Figure 9c for the nearby point at Delihalil) is subtracted from the same $\sim 7 \text{ mm a}^{-1}$ northward velocity of the stable interior of the African plate relative to Eurasia.

The oceanic spreading in the Red Sea probably initiated in the latest Oligocene or earliest Miocene as a result of forces exerted on the overlying lithosphere by the Afar mantle plume (e.g., Westaway 1993). It is evident that once this spreading system began to develop, both the crust and the mantle lithosphere of Arabia were required to move anticlockwise relative to Africa. Since no subduction system existed at this time along the northern margin of Arabia that could conserve mantle lithosphere volume, the only feasible geometry for the mantle lithosphere motion to have adopted is for its motion relative to Africa to decrease northward and westward, beneath Turkey (Figure 11a) (and also to decrease northward, farther east, beneath the Caucasus region; although the detailed motion geometry there is beyond the scope of this study). Shear tractions exerted on the brittle upper crust by the resulting component of mantle lithosphere shortening can indeed readily account for the widespread evidence of distributed crustal shortening occurring across much of Turkey at this time (e.g., Westaway & Arger 2001).

As far as the brittle upper crust is concerned, the simplest feasible geometry that could have developed at this time would have been a left-lateral fault zone that started along the line of the southern DSFZ but then continued offshore, northwestward (Figure 12), rather than stepping to the right across Lebanon as the real DSFZ did. Such a geometry would have minimised the relative horizontal motions between the brittle upper

crust and underlying mantle lithosphere. To account for the fact that this did not happen, it is suggested that this African “promontory” is an instance where upper-crustal and mantle-lithosphere velocities are NOT significantly decoupled. This could be due either to the thinness of the continental crust here, consistent with the deep ($\sim 2 \text{ km}$) bathymetry (e.g., Kempler & Garfunkel 1994; Vidal *et al.* 2000), which may reduce or eliminate any weak lower-crustal layer. It may instead be due to the presence at depth of substantial bodies of mafic ophiolitic material, which are not expected to flow at normal lower-crustal temperatures. As already noted, another possible reason, suggested by Lovelock (1984) and Walley (1998), is that NNE-trending fault zones already existed in Lebanon, Syria, and southern Turkey, as a result of earlier crustal deformation, such as during the latest Cretaceous ophiolite obduction. It can be presumed to have been mechanically easier to reactivate such structures within stepover zones along the DSFZ than to have created new fault segments with a more optimal orientation relative to the imposed motions in the mantle lithosphere. As a result, the central and northern DSFZ developed as a series of N–S- and NNE–SSW-trending left-lateral fault segments that form the internal faults within transpressive stepovers (Figure 11a). As one moves north, these faults become increasingly misaligned relative to the underlying motion in the mantle lithosphere. During the Miocene, the component of left-lateral slip can thus be presumed to have gradually decreased northward, as the component of distributed shortening gradually increased (Figure 11a). This zone of transpression can thus be presumed to have gradually died out into the zone of distributed shortening within Turkey that existed during the Miocene and has already been mentioned.

The picture that thus emerges for the kinematics of the “triple junction” between Africa, Arabia, and Turkey is illustrated in Figure 11 and its caption. Once oceanic spreading began in the Red Sea, a fault zone became required in the Levant region to accommodate the difference in relative velocity between the brittle upper crust in the African and Arabian plates. The optimum orientation would appear to have been something like in Figure 12. It presumably did not develop because it was mechanically easier for the actual DSFZ to develop in the weaker crust farther east, even though this meant that it was not optimally oriented for transform faulting –

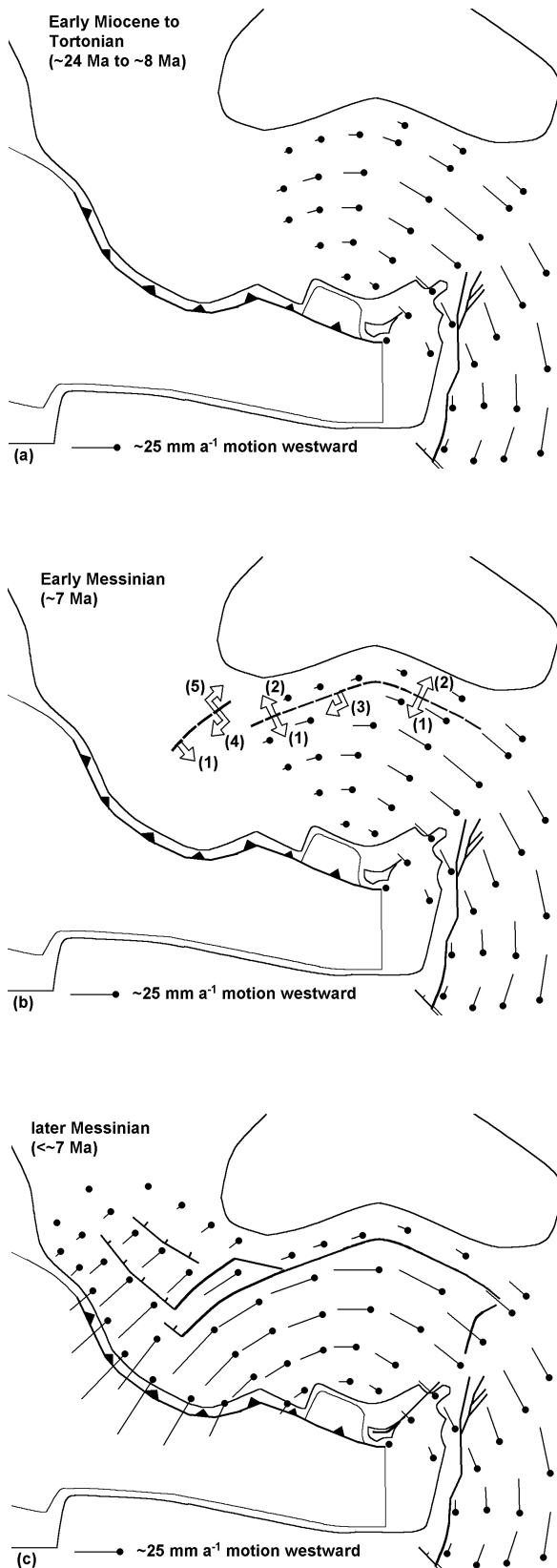


Figure 11. Cartoons summarising the suggested evolution of the mantle lithosphere flow pattern in the study region in relation to the most important active faults affecting the brittle layer. (a) During the Early Miocene to Tortonian, oceanic spreading was occurring in the Red Sea and the DSFZ was active. The anticlockwise mantle flow beneath Arabia, required to accommodate the Red Sea spreading, gradually died out westward beneath Turkey. The associated component of east-west convergence across the mantle lithosphere beneath Turkey imparted shear tractions on the base of the brittle layer in a sense consistent with SE–NW or E–W crustal shortening, consistent with the widespread distributed shortening occurring in this region at this time. The present phase of Aegean extension had not yet begun. Subduction of the African plate along the Hellenic subduction zone was already occurring but the location of the trench was stable: no rollback of the surface trace of the subduction zone was occurring. (b) The dramatic fall in sea level in the Mediterranean (and arguably also in the Black Sea) in the Early Messinian caused a dramatic reduction in the horizontal stress acting on the brittle upper crust and mantle lithosphere of Turkey. The main effects on the brittle layer are estimated, at the positions indicated, to have been as follows. First, a reduction in the normal stress across the line of the incipient NAFZ caused by the fall in sea level in the Mediterranean (1) and Black Sea (2). Second, the development of component of right-lateral shear stress across the line of the incipient NAFZ caused by the pre-existing westward component of motion of the brittle upper crust in central-eastern Turkey caused by the pre-existing mantle lithosphere flow (3). Third, the development of component of right-lateral shear stress across the line of the incipient western NAFZ caused by the fall in sea level in the part of the Mediterranean Sea adjacent to the western part of the Hellenic subduction zone (4) and in the western Black Sea (5). It is assumed that the combined effect of these contributions created the conditions for right-lateral shear failure along the line of the NAFZ. (c) As soon as the NAFZ became active, the brittle layer of the new Turkish plate was able to move anticlockwise relative to Eurasia as a unit. The MOFZ and MKFZ came into being to form the eastern margin of this new plate, the geometry of their initial linkage to each other and to the DSFZ (not shown) being discussed in the text and by Westaway & Arger (1996, 2001). With the brittle layer of the Turkish plate now moving westward as a unit, the shear traction that formerly acted between it and the underlying mantle lithosphere (which drove the pre-existing shortening of the upper crust and caused the mantle lithosphere shortening to die out westward, in (a), disappeared. As a result, the mantle lithosphere beneath Turkey now became able to flow southwestward right up to the Hellenic subduction zone. This meant that the surface trace of this subduction zone became free to begin to roll back SW. The resulting reduction in horizontal stress along the SW margin of the overlying lithosphere required the start of local extension. Most of the NAFZ is thus located above a zone of abrupt right-lateral velocity gradient in the underlying mantle lithosphere. In the Aegean region, the requirement of the crust and mantle lithosphere to accommodate both right-lateral slip on the NAFZ and rollback of the subduction zone leads to a gentler NW tapering in SW velocity in both, explaining the width of the zone of Aegean extension NW of the western NAFZ. A similar geometry of mantle lithosphere flow (not shown) is assumed to persist to the present day, although the geometry of the left-lateral faults in the brittle upper crust, forming the eastern margin of the Turkish plate, has changed substantially (see text).



Figure 12. Schematic ideal initial geometry for the DSFZ in the absence of lateral variations in crustal strength and possible pre-existing lines of weakness along its line. See text for discussion.

necessitating the observed complicated sequence of transpressional stepover segments. Farther north, this non-optimally oriented fault zone encountered the Hatay ophiolite. The greater complexity (Figures 2 & 3) that developed there involves strike-slip fault segments reactivating – or intersecting at a low angle (Figure 7) – older structures inherited from the time of ophiolite obduction (e.g., Çoşkun & Çoşkun 2000). This complexity thus presumably also relates to the greater local strength of the crust, due the presence of so much mafic material: the strike-slip faulting that developed in the Miocene was presumably obliged to follow pre-existing lines of weakness through these strong areas. The associated flow of mantle lithosphere away from the Dead Sea spreading centre is instead estimated to have been northwestward, to beneath Turkey, rather than parallel to the DSFZ.

In the present-day pattern of deformation (Figure 11c), viewed from the perspective of the Turkish plate, the northwestward flow of mantle lithosphere from beneath Arabia imparts shear tractions on the brittle layer which maintain the observed motion relative to Eurasia, opposing the frictional forces exerted across the NAFZ. The EAFZ allows this block of brittle upper crust to move relative to the brittle upper crust of Arabia: being brittle, its velocity presumably cannot vary smoothly in a continuous manner from the interior of Arabia like appears to be possible within the mantle lithosphere.

Viewed instead from the perspective of the African plate, this plate is “trying” to move northward relative to Eurasia. However, the northwestward flow of mantle

lithosphere beneath the “promontory” of the African plate east of Cyprus is relatively well coupled to the brittle layer in this region, causing this promontory to be deflected towards the NW. The resulting component of convergence between the crust of this promontory and the southern margin of the Turkish plate is presumably responsible for the complexity of the observed deformation around İskenderun Gulf. This convergent motion acting on this relatively strong block of crust containing much ophiolitic material can be assumed to have increased the normal stress across the Karataş-Osmaniye Fault to such an extent that it can no longer slip, forcing slip to have migrated northward onto the Yakapınar-Göksun Fault. At the same time, this relatively strong block is being forced to rotate anticlockwise, rather like a ball-bearing, or experiencing an equivalent sense of distributed simple shear (Figure 8b), causing the patterns of relative motion evidenced by GPS (Figure 8a). Supporting evidence for this view is provided by analysis of the Ceyhan earthquake of 27 June 1998 ($M_w=6.2$), which occurred near the southern end of the Yakapınar-Göksun Fault. This event and its aftershocks occurred at the depth range of ~20–40 km (Aktar *et al.* 2000), indicating brittle behaviour at an unusually great depth.

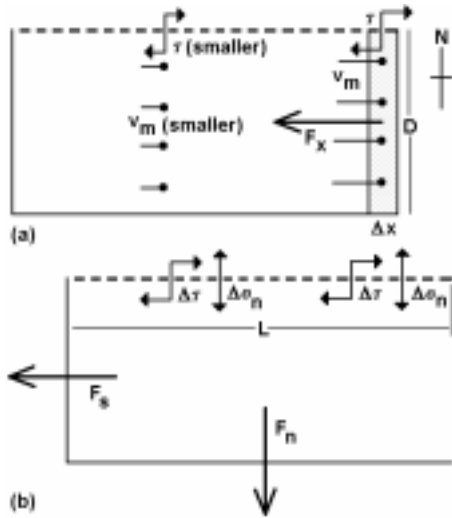
Discussion

The Initiation of the NAFZ

The geometry of relative motions in Figure 11a requires substantial relative horizontal motions between the brittle upper crust and mantle lithosphere beneath Turkey, with the motion of the mantle lithosphere acting to try to shear the brittle upper crust towards the west. Consider the westward force F_x acting on a vertical section of the brittle upper crust with N–S length D and width Δx (Figure 13a). The westward shear traction s_{xz} applied to each unit area of the base of the brittle layer can be estimated as

$$\Delta_{xz} = \eta_e v_m / W \quad (2)$$

(e.g., Westaway 1998), where η_e is the effective viscosity of the lower crust, v_m the relative horizontal velocity between the brittle upper crust and the mantle lithosphere, and W (~15 km) is the thickness of the lower crust. This traction will be largest in the vicinity of where the initial eastern end of the NAFZ later developed, near

Figure 13^(*)

Erzincan, as v_m is locally expected to be largest there. A test of the feasibility of the scheme in Figure 11(a) is thus that it does NOT predict the NAFZ developing in the vicinity of Erzincan as soon as oceanic spreading began in the Dead Sea. The resulting force F_x acting on an element of brittle upper crust with dimensions D (N–S; ~ 400 km) and Δx (E–W) will thus equal

$$F_x = \sigma_{xz} D \Delta x = \frac{\eta_e v_m D \Delta x}{W} \quad (3)$$

The critical condition is whether such a force can cause shear failure at the base of the brittle layer (depth z_b), to form a new fault plane. To test this, I use the Coulomb-Navier failure criterion, for which the condition for no failure can be expressed (e.g., Westaway 1999a) in the form

$$\Phi < 0 \quad (4)$$

where Φ , the failure parameter, is given by

$$\Phi = |\tau| - (S + \mu' \sigma_n) \quad (5)$$

S (~ 100 MPa) and μ' (~ 0.5) being the cohesion and coefficient of internal friction of intact rock, and σ_n and τ being the normal stress and shear stress resolved onto the failure plane. For the geometry in Figure 13a, σ_n at depth z_b can be estimated roughly as the lithostatic stress minus the pore fluid pressure:

$$\sigma_n = (\rho_c - \rho_w) g z_b, \quad (6)$$

where ρ_c (~ 2700 kg m⁻³) and ρ_w (~ 1000 kg m⁻³) are the densities of crustal rock and pore water, and g (~ 9.81 m s⁻²) is the acceleration due to gravity. If there is no failure, the shear stress τ , summed across all depths from 0 to z_b for a patch of fault with E–W width Δx , must balance the force F_x calculated in equation (3). This requires the mean value of τ , vertically averaged across the brittle layer, to equal $F_x / \Delta x z_b$. However, if τ is assumed to match this spatial average by increasing linearly across the brittle layer from 0 at the Earth's surface, its value at the base of the brittle layer will be

$$\tau = 2 F_x \Delta x z_b \quad (7)$$

Substituting from (3), (6) and (7) into (5), and using (4), the condition for no shear failure can be written as

$$\eta_e < \frac{z_b W}{2 v_m D} (S + \mu' (\rho_c - \rho_w) g z_b) \quad (8)$$

and can be solved for $v_m \sim 25$ mm a⁻¹ to yield $\eta_e < \sim 8 \times 10^{19}$ Pa s.

The reduction in Mediterranean water level by a distance H (~ 3 km) during the Messinian (starting at ~ 7.1 Ma) reduced the water load and the lithostatic pressure in the underlying crust, and so caused a force, F_i , to develop, acting outwards from the original land area, perpendicular to each segment of coastline. The length, X , of the part of the Mediterranean coastline between NW Greece and the northern end of the Levant coastline, after the curvature resulting from post-

(*)Figure 13. Schematic plan views of Turkey indicating the stress mechanics governing the initiation of the NAFZ. (a) In the Middle Miocene, the westward mantle flow (at velocity v_m) applied a westward shear traction to the base of the brittle layer. As v_m decreased westward (Figure 11a) this traction was largest in the east, and caused the westward force F_x to act on the "critical element" of upper crust whose northern end was located near Erzincan. This force resulted in a component of shear stress τ across the line of the future NAFZ (thick dashed line), but this was insufficient to initiate shear failure, even at the "critical element". (b) The unloading of the crust to the south and west during the Messinian regression led to forces F_n and F_s acting on the brittle upper crust of Turkey in directions normal and tangential to the line of the future NAFZ. Force F_n caused a reduction in the normal stress by $\Delta\sigma_n$ across the line of the NAFZ; force F_s caused an increase $\Delta\tau$ in the shear stress across this line. In combination with the stress field already in existence in (a), these changes were sufficient to initiate shear failure along the line of the NAFZ. Once it formed, the block of brittle upper crust to the south was free to move westward, roughly at the same rate as the underlying mantle lithosphere flow, which was then able to persist westward as in Figure 11c.

Miocene Aegean extension is restored (Figure 11) can be estimated as ~1500 km. Simple integration indicates that the magnitude of F_i (summing, for the time being, all contributions as a scalar, regardless of orientation) can be estimated as

$$F_i = \rho_c g X H^2 / 2 + \rho_c g X (H z_b - H^2) \quad (9)$$

where the first term represents the direct effect of water removal and the second term represents the resulting reduction in lithostatic pressure in the underlying crust. Equation (9) can thus be simplified as

$$F_i = \rho_c g X (H z_b - H^2 / 2) \quad (10)$$

allowing F_i to be evaluated as $\sim 1.6 \times 10^{18}$ N.

Some studies (e.g., Hsü & Giavanoli 1979) have suggested that the Black Sea also regressed during the Messinian. Taking the estimated amount of regression, H , as ~1 km and the length of the southern Black Sea coastline, X , as ~1200 km, one obtains from (10) an additional contribution to F_i of $\sim 0.5 \times 10^{18}$ N.

Given the geometry, when resolved along the line of the future NAFZ the total of F_i can be assumed partitioned into a component F_n of $\sim 1.0 \times 10^{18}$ N oriented so as to reduce the normal stress and a component F_s of $\sim 0.5 \times 10^{18}$ N oriented so as to increase the right-lateral shear stress (Figures 11b & 13b) (plus other components in senses that would leave the state of stress on the future NAFZ unaffected).

The component F_n will cause a spatially averaged reduction in N-S horizontal stress along the future NAFZ of $F_n / (z_b L)$, L (~1200 km) being the initial length of the NAFZ (measured from Erzincan to the central Aegean Sea). Assuming as before that this component is partitioned vertically so it increases from zero at the Earth's surface to double the spatial average at the base of the brittle layer, the corresponding change in normal stress at the base of the brittle layer $\Delta\sigma_n$ can be estimated as

$$\Delta\sigma_n = \frac{2 F_n}{z_b L} \quad (11)$$

and is estimated as ~110 MPa. Likewise, the corresponding increase in right-lateral shear stress, $\Delta\tau$, can be estimated as

$$\Delta\tau = \frac{2 F_s}{z_b L} \quad (12)$$

and is ~55 MPa.

The condition for shear failure now occurring at the critical point (equation (5)) thus adjusts to

$$|\tau + \Delta\tau| - (S + \mu' \sigma_n + \mu' \Delta\sigma_n) > 0 \quad (13)$$

or

$$\eta_e > \frac{z_b W}{2v_m D} \left[(S + \mu'(\rho_c - \rho_w)g z_b) - \left(\frac{2(\mu' F_n + F_s)}{z_b L} \right) \right] \quad (14)$$

and can be solved for $v_m \sim 25 \text{ mm a}^{-1}$, as before, to yield $\eta_e > \sim 4 \times 10^{19}$ Pa s. Once the initial eastern end of the NAFZ developed, the associated fracture through the brittle upper crust can be expected to have propagated rapidly westward. Thus, although it now seems clear that the NAFZ initiated in the east (as is usually assumed), one does not now expect any significant interval between its development there and its first appearance in the Aegean region.

Of course, if the NAFZ developed during the Early Messinian sea level fall, rather than at the peak of the regression, smaller values of F_n and F_s should be used in (14), increasing the estimated lower bound to η_e . On the other hand, these crude calculations also neglect the fact that some parts of the NAFZ, such as along the North Aegean Trough, follow fault segments that already existed in Messinian time (e.g., Le Pichon *et al.* 1984). The incipient NAFZ in the Gallipoli region of NW Turkey (Gelibolu; Figure 1) also seems to have reactivated part of an ancient fault line along the suture of the intra-Pontide ocean (e.g., Tüysüz *et al.* 1998). It can be presumed to have been mechanically easier to reactivate these pre-existing faults with a component of right-lateral slip than to create new right-lateral faults through previously intact rock. The effect of this omission can be roughly incorporated by replacing the value of S , the cohesion of rock, that is used in the calculations with a number that is somewhere between the 100 MPa value for intact rock and 0 for a pre-existing fault plane. The effect of this would be to reduce the values of both the upper and lower bounds to η_e estimated in equations (8) and (14). These two potential causes of systematic error will of course partly cancel out, at least for estimation of the lower bound to η_e from equation (13). Since this lower bound cannot exceed the upper bound from equation (7), one may conclude that the bulk of the ~3-km regression in the Mediterranean Sea was necessary to create the conditions to initiate the NAFZ. The estimate of $L=1200$ km is of course an upper bound, assuming that none of

the incipient NAFZ followed any pre-existing fault zone. This seems to be a reasonable assumption for most of the NAFZ located onshore to the east of the Sea of Marmara. However, removing the lengths of fault from Gallipoli westward from the calculation reduces L to ~ 800 km, which from equation (13) indicates $\eta_e > \sim 2 \times 10^{19}$ Pa s.

For comparison with these viscosity estimates, heat flow data for central and western Turkey (e.g., Ilkışık 1995; Ilkışık *et al.* 1997; Pfister *et al.* 1998) predict a Moho temperature in the region of ~ 600 °C. Given Westaway's (1998) preferred viscosity parameterisation, this would suggest $\eta_e \sim 1 \times 10^{19}$ Pa s. However, lower heat flow is expected before the present phase of extension, when the mantle lithosphere was thicker, and so this viscosity estimate is a lower bound. In contrast, Westaway (2002b) estimated the present-day η_e beneath the Gulf of Corinth in central Greece as $\sim 6 \times 10^{19}$ Pa s. Approximations in the technique used suggest that this estimate is an upper bound for this region. However, its agreement with the range of η_e of $\sim 2 \times 10^{19}$ Pa s to $\sim 8 \times 10^{19}$ Pa s required for the non-existence of the NAFZ before the Messinian (equation 8) and its appearance during the Messinian (equation 14) suggests that it is not far wide of the mark.

The NAFZ can thus be regarded as forming along the line where the combined effects of the shearing of the brittle layer by the pre-existing westward motion of the underlying mantle lithosphere and the increased shearing effect and reduction in normal stress caused by the Messinian regression were greatest. Once the NAFZ formed, the block of brittle upper crust to the south of it was free to move westward, rotating anticlockwise about the NAFZ Euler pole, at a rate that is presumed to roughly match the original sense and rate of mantle lithosphere flow along its eastern margin. The horizontal motions in the underlying mantle lithosphere were now able to persist westward, as shown in Figure 11c, rather than dying out as in Figure 11a. As a result, after the initiation of the NAFZ, the magnitude of relative horizontal motions between the brittle upper crust and the underlying mantle lithosphere in what was now the Turkish plate were much smaller than before. It can be presumed that the mantle flow velocity in this sense exceeds the upper-crustal velocity by an amount which, spatially averaged, is sufficient to make the magnitude of the force term F_x large enough to overcome the frictional stress across the NAFZ.

This reasoning can also explain the principal irregularity along the NAFZ – the major rightward step of its main strand across the Sea of Marmara pull-apart basin (Figure 1). Once the NAFZ propagated westward to this longitude, it would have “lost” any effect of reduction in the normal stress caused by regression in the Black Sea, and also most likely “lost” any significant pre-existing shearing effect of the underlying mantle lithosphere (as this can be presumed to have largely died out farther east; Figure 11a). Its rightward step at this point allowed a greater proportion of the Mediterranean coastline to exert force components that contributed to maintaining the reduced normal stress and increased shear stress required to satisfy the failure criterion. However, another relevant factor – already mentioned – was presumably that in this region the incipient NAFZ could develop by reactivating the pre-existing line of weakness along the intra-Pontide suture. This possibility (Tüysüz *et al.* 1998) suggests that even though this suture did not have precisely the correct orientation for a NAFZ strand, it was mechanically easier to reactivate it in a right-lateral sense than for a new right-lateral fault segment with the optimal orientation to develop. More detailed analysis of the geometry of this part of the NAFZ in future may thus improve constraint on η_e for this region. In the meantime, it will be necessary to improve constraint on the magnitude of the Black Sea regression that occurred in the Messinian (the Pontian stage of the local Black Sea stratigraphy).

It is presumed that the initiation of the NAFZ was accompanied by the development of the conjugate left-lateral MOFZ, and by the Misis-Kyrenia Fault Zone, as shown schematically in Figure 11c. The Misis-Kyrenia Fault Zone is likewise assumed to have propagated NE across southern Turkey, forming the Karataş-Osmaniye Fault and linking up with the various left-lateral fault strands that formed the initial northern end of the DSFZ. The MOFZ is likewise assumed to have propagated SSW across eastern Turkey towards these other fault zones.

As already noted, the MOFZ was subsequently superseded (probably at ~ 4 Ma) by the modern EAFZ. The Karataş-Osmaniye Fault also appears to have later been superseded by the Yakapınar-Göksun Fault. As already discussed, it is unclear whether these two events were synchronous. One possibility is thus that the “jamming” of relatively strong ophiolitic crust against the Karataş-Osmaniye Fault, which seems to have locked it

up, initiated a reorganisation of left-lateral faulting throughout the region. Another possibility, suggested by Westaway & Arger (2001), is that the MOFZ was superseded due to the geometry of its intersection with the NAFZ near Erzincan being unable to accommodate large amounts of slip. At present, the age control evidence is insufficient to establish the relative order of these two events: further work is needed.

It has previously been suggested (e.g., by Şengör *et al.* 1985) that the NAFZ is a characteristic “tectonic escape” structure that developed in order to accommodate AR-EU convergence by allowing the “wedge” comprising the Turkish plate to move westward away from this convergent zone, towards the “free surface” facing the Hellenic subduction zone. The present analysis suggests that the situation is rather more complex. First, the contribution of plate convergence to initiating the NAFZ was via the shear traction exerted on the base of the brittle upper crust of the Turkish plate by the relative motion of the Arabian mantle lithosphere, not by any “contact force” applied directly through the brittle upper crust. Second, this shear traction on its own was insufficient to initiate the NAFZ: it required the additional effect of the changes in the stress field that accompanied the Messinian drawdown in Mediterranean sea level. In this sense, the NAFZ is a unique structure that owes its existence to a local coincidence: it thus represents an extreme example of the ability of climate to affect crustal deformation. However, had the AR-EU convergence between ~50% faster – say, ~40 mm a⁻¹ instead of ~25 mm a⁻¹ – the earlier calculations indicate that, once the Red Sea spreading centre came into being, the shear traction applied to the “critical element” of Turkish crust would have been large enough to initiate shear failure along the line of the NAFZ, enabling this fault zone to have come into being in the Early Miocene. The physical mechanism suggested in Figure 11a may thus be applicable for explaining other instances of strike-slip faulting during “tectonic escape” in regions where plate convergence is faster, or the lower-crustal effective viscosity is lower, than in the eastern Mediterranean region. The main global implication of the NAFZ is its usefulness for constraining the effective viscosity of the lower continental crust of Turkey. As this crust is not atypical, the resulting estimate, $\sim 5 \pm 3 \times 10^{19}$ Pa s, can be considered appropriate for many other regions as well as for Turkey itself.

Coupling between the NAFZ and the Turkey-Africa Plate Boundary

The proposed regional kinematic model suggests that the modern strike-slip boundaries of the Turkish plate are in almost all cases optimally oriented subparallel to the local plate motions. The main exception is in the vicinity of İskenderun Gulf. In this vicinity, it has been suggested that the Karataş-Osmaniye Fault, which is optimally oriented, has become locked, requiring a combination of distributed deformation and slip on the Yakapınar-Göksun Fault farther north. It has been suggested that this difficulty results from the presence within the plate boundary zone of ophiolitic crust that has relatively high strength and – due to its probable lack of a plastic lower-crustal channel – is required to move with the underlying mantle lithosphere. The presence of this localised patch of high-strength crust thus appears to have increased the normal stress across the Karataş-Osmaniye Fault, preventing continued slip on it.

The overall kinematic consistency of the regional model nonetheless requires slow deformation in this vicinity in order to enable the specified relative motions to occur, including slip on the NAFZ. However, achieving this local deformation is relatively difficult, due to the high strength of the crust. It thus appears reasonable to regard this locality as a kind of “geometrical lock” whose deformation permits relative motion between the surrounding plates. Regarding this hypothesis, it is interesting to note that the Ceyhan earthquake of 27 June 1998 ($M_s=6.3$) preceded the larger earthquakes on the western NAFZ in late 1999. This is consistent with the view that a small fault movement in the Ceyhan area changed the regional state of stress so as to enable a much larger amount of slip to occur on part of the western NAFZ, consistent with the 1998 earthquake being a “trigger” or “precursor” of the 1999 events.

However, earlier instances of temporal correlation between earthquakes on the NAFZ and on the TR-AF plate boundary are somewhat different. The 9 August 1912 Saros-Marmara earthquake on the western NAFZ ($M_s \sim 7.4$; Ambraseys 1988) was followed by the 29 September 1918 earthquake ($M_s \sim 6.8$; Ambraseys 1988) in (or just offshore of) eastern Cyprus. This was followed in turn by the 9 June 1919. Cerkeş-Tokat earthquake ($M_s \sim 5.9$; Ambraseys 1988) on the central NAFZ and later by the larger 18 November 1919 Soma

normal-faulting earthquake ($M_s \sim 6.9$; Ambraseys 1988) just south of the western NAFZ. The 26 December 1939 Erzincan earthquake on the eastern NAFZ ($M_s \sim 7.8$; Ambraseys 1988) preceded the eastern Cyprus earthquake of 20 January 1941 ($M_s = 5.9$; Ambraseys 1988), which in turn preceded the sequence of larger events on the central and western NAFZ in 1942–1944. Detailed monitoring of the seismicity and crustal deformation occurring around İskenderun Gulf may thus provide the basis of a warning mechanism for future destructive earthquakes in densely populated localities along the NAFZ.

Relationship to Plate Tectonics

It is evident that the present study, proposing significant horizontal relative motions between the brittle upper continental crust and the mantle lithosphere, is not in strict accordance with plate tectonics. In particular, the “Turkish plate” is not a plate in the strict sense of the term: its proposed mantle lithosphere boundaries relative to the neighbouring Eurasian and Arabian plates are just zones of velocity gradients rather than localised discontinuities. The EAFZ indeed seems to be a purely upper-crustal feature, which only exists because the brittle upper crust cannot deform continuously as it passes around the “corner” in the northeastern Mediterranean; whereas the mantle lithosphere can.

As already noted, the possibility of such relative horizontal motions follows from the presence of the weak lower-crustal layer. Such effects will, however, be absent in most other regions of continental lithosphere, because most plates are larger and contain one or more Archaean cratons. In such regions, where the heat flow is low due in part to chemical differences and in part to abnormally thick mantle lithosphere (e.g., Westaway 1995b), the brittle upper crust is bonded to the mantle lithosphere. Such regions will, in effect, “pin” the brittle upper crust to the mantle lithosphere throughout the rest of each plate, at least as far as horizontal relative motions are concerned. In contrast, the crust of the Turkish and Arabian plates consolidated in the Late Precambrian (the Pan-African orogeny) (e.g., Arger *et al.* 2000). No Archaean cratons are thus present, and significant relative motions are also facilitated by the relative smallness of these plates, which reduces the magnitude of the horizontal shearing force required to maintain a given rate of horizontal relative motion.

In contrast, relative *vertical* crustal motions between the brittle upper crust and mantle lithosphere, associated with inflow or outflow of lower crust, are very widespread in the geological record (e.g., Arger *et al.* 2000; Westaway 2001, 2002b, c, d; Westaway *et al.* 2002, 2003; Bridgland *et al.* 2003). As Westaway *et al.* (2002) have pointed out, the typically low flexural rigidity of the brittle upper crust means that it is free to flex to accommodate such motions, and this remains true even if some parts of it are “pinned” both vertically and horizontally by Archaean cratons or other strong patches. There is thus no contradiction between the widespread presence of vertical relative motions and the much greater degree of stability towards relative horizontal motions that is evident in most regions of continental crust and allows plate tectonics to usually work pretty well within the continents despite the presence of the weak lower-crustal layer. Indeed, estimates of the lower-crustal effective viscosity derived from vertical relative motions (e.g., Westaway 2001, 2002b, d; Westaway *et al.* 2002) and horizontal relative motions (this study) are in good agreement.

Nonetheless, to avoid future semantic difficulties I suggest that a term is needed to describe regions of upper crust with little or no internal deformation, such as within the Turkish and Arabian “plates”, which are not necessarily moving in step with the underlying mantle lithosphere. I suggest calling them upper-crustal “rafts”. One could thus summarise the present study region by stating that “Oceanic spreading between the African and Arabian plates, in the Red Sea, requires anticlockwise motion of the Arabian mantle lithosphere relative to Eurasia. This relative motion persists as far as the surface trace of the Hellenic subduction zone, where the African mantle lithosphere is rolling back southward away from the overriding Arabian mantle lithosphere. The Arabian mantle lithosphere supports two principal “rafts” of relatively stable upper crust, the Turkish and Arabian “rafts”, which are both moving anticlockwise relative to Africa but whose minor motions relative to each other are accommodated on the EAFZ”.

Future Refinements to the Regional Kinematics

The model derived in this study indicates that the present-day kinematics of the study region are now quite tightly constrained. For Turkey, the discrepancies that remain – notably, the difference between the geological and geodetic estimates of slip and slip rate on the NAFZ –

have been tentatively explained. More issues remain unresolved within Syria, reflecting the relative lack of research there compared with in Turkey. These include, as already discussed, the manner of partitioning of left-lateral slip across the zone of en-echelon faults in northern Syria. Also, the extent to which this may have changed systematically over time remains unresolved: for instance, it remains possible that most – if not all – of the slip on the Afrin Fault, linking northward into the array of en-echelon faults in the Gaziantep area (Figure 2), may have occurred in the Miocene and earliest Pliocene; this system possibly becoming effectively “abandoned” when the throughgoing linkage between the DSFZ and EAFZ came into being in the Early Pliocene. A second issue concerns the importance of distributed left-lateral simple shear and SE–NW shortening in the Palmyra fold belt. If the relative rotation rate across the DSFZ in southern Syria were, for instance, reduced to $0.21^\circ \text{ Ma}^{-1}$, then the slip rate on the Masyaf Fault predicted from it would decrease to 3.38 mm a^{-1} , requiring 17 km of left-lateral offset of the Homs Basalt since 5 Ma. This would require a shortening rate of 1.34 mm a^{-1} across the Palmyra fold belt, requiring ~ 25 km of shortening since 19 Ma. This adjustment would also reduce the predicted rate of left-lateral slip at the latitude of the Karasu Valley to $\sim 2.5 \text{ mm a}^{-1}$, closer to the range of estimates of the slip rate on the Amanos Fault obtained by Yurtmen *et al.* (2002).

Consideration of kinematic consistency between SE Turkey and Syria also raises another question: whether the shortening in the Palmyra fold belt dies out northeastward, whether it continues into a zone of active SE–NW shortening in the Sinjar fold belt in the Syria-Iraq border region (Figure 1), or whether it possibly transfers onto a component of left-lateral slip on the SE–NW-trending Al Furat Fault in central-northern Syria (Figure 1). If the latter is happening, one would expect this component of relative plate motion to somehow couple back into the other strands of the AF-AR and/or TR-AR plate boundaries in the Gaziantep area of southeast Turkey. Such a scheme would permit the existing kinematic model for the EAFZ (Figure 9a & b) to be reconciled with a lower slip rate on the DSFZ in Syria and in the Karasu Valley. A final uncertainty is, of course, that if the Palmyra fold belt is linked via other structures to the northern margin of the Arabian plate, then the area north of it should be regarded as a separate, “Syrian”, plate (SY), rotating relative to Arabia. If so, the SY-AF Euler pole would be expected to not coincide with the AR-

AF pole, and would require a separate determination using local evidence. This possibility should ultimately be resolvable using GPS. However, in the meantime, because any SY-AR relative motions are evidently small compared with the AF-AR relative motions, the existing scheme can serve as a reasonable approximation. Regarding this scheme, it is worth noting that the McClusky *et al.* (2002) reference frame for the Arabian plate was determined using three GPS points in southern Turkey (GAZI, and two others farther east), plus a fourth point located many hundreds of kilometres to the south and east in Bahrain. The consistency between these points suggests that no major throughgoing zone of shortening cuts across this plate. However, from earlier discussion, the likely upper bound to the shortening rate across the Sinjar fold belt (Figure 1) is only $\sim 1 \text{ mm a}^{-1}$, a rate of relative motion that would probably not be resolvable using the available GPS data.

Recent trenching work at El Harif, ~ 5 km north of the town of Masyaf, suggests an additional constraint on the present-day kinematics (Meghraoui 2002). The DSFZ has particularly simple form in this locality, with only a single active strand, which offsets an aqueduct – of Hellenistic or Roman origin – by 13.6 m. This trenching indicates that this structure has been offset by three earthquakes. The first of these, involving a 4.5-m offset, seems to have occurred not long after the aqueduct was built, being radiocarbon dated to no older than 210 BC. Radiocarbon dating also indicates that the final event occurred just under 1000 years ago, enabling it to be associated with the destructive historical earthquake of 29 June 1170 (e.g., Ben-Menahem 1981; Ambraseys & Barazangi 1989). Earlier major earthquakes are known on the DSFZ in Syria, for instance in A.D. 859, 500, 245 and 115, and 63 B.C. (e.g., Ben-Menahem 1981), but it is unclear at this stage which were responsible for the initial two offsets of this aqueduct. The local slip rate can thus be estimated as $13.6 \text{ m} / 2212 \text{ a}$ or 6.15 mm a^{-1} . The true rate may be higher than this figure, if the first earthquake occurred well after 210 B.C., or lower, if the next earthquake does not occur for centuries in the future. Meghraoui (2002) estimated that the true slip rate probably lies within the range $\sim 5.5\text{--}7.0 \text{ mm a}^{-1}$. For instance, if the initial offset is assumed to have occurred in 63 B.C., the subsequent time-averaged slip rate can be estimated as $\sim 13.6 \text{ m} / 2065 \text{ a}$ or 6.59 mm a^{-1} . Such a slip rate would indicate an AF-AR rotation rate of 0.42°

Ma^{-1} . Such a rate would require left-lateral slip at $\sim 6 \text{ mm a}^{-1}$ on the southern DSFZ, the upper bound permitted by the available evidence, even if no shortening is assumed to be occurring across the Palmyra fold belt. It would also require an overall rate of left-lateral simple shear of $\sim 5 \text{ mm a}^{-1}$ across the AF-AR plate boundary at the latitude of Hatay, which would imply a component of slip on the Afrin Fault and/or a component of distributed left-lateral simple shear in addition to the left-lateral slip on the Amanos and East Hatay faults.

The most important issue in this study region would appear to be to determine a definitive age for the NAFZ, to allow testing of the proposed physical model (Figure 11).

Conclusions

A revised kinematic model has been determined for the present-day relative plate motions in the eastern Mediterranean and Middle Eastern regions, based on a combination of geological and GPS data. The relative motions of the brittle upper crust of the African and Arabian plates across the southern DSFZ are represented by relative rotation at $0.278^\circ \text{ Ma}^{-1}$ about an Euler pole at $31.1^\circ \text{N } 26.7^\circ \text{E}$. The resulting predicted slip rate on the southern DSFZ is 4.0 mm a^{-1} . The kinematics of the northern DSFZ are described as relative rotation at $0.243^\circ \text{ Ma}^{-1}$ about the same Euler pole, the difference in rotation rates reflecting the absorption of a small component of the relative plate motion by distributed shortening in the Palmyra fold belt. The northern DSFZ, in Syria and southern Turkey, is regarded as a series of transpressional stepovers, along which the rate of left-lateral slip is substantially less than the rate of relative plate motion, because this slip is oriented strongly obliquely to the relative motion between the adjoining plates. This geometry seems to result in part from some strands of the northern DSFZ reactivating older fault segments, even though they were not optimally oriented relative to the AF-AR plate motion, and in part because its ideal initial geometry (Figure 11) was precluded by the high strength of the crust offshore of the Levant coastline.

The revised slip rate on the EAFZ is estimated as $\sim 8 \text{ mm a}^{-1}$. At this rate, restoring the observed slip requires the age of the EAFZ to be $\sim 4 \text{ Ma}$. The previous phase of deformation (Westaway & Arger 2001), which involved slip on the MOFZ before the EAFZ came into being, is

thus dated to $\sim 7\text{--}4 \text{ Ma}$, suggesting a timing of initiation for the NAFZ of $\sim 7 \text{ Ma}$, not $\sim 5 \text{ Ma}$ as has previously been thought. Local evidence from the western NAFZ also supports a $\sim 7 \text{ Ma}$ or Early Messinian age for the NAFZ. The overall present-day kinematics of the NAFZ are described using the Euler vector determined by McClusky *et al.* (2000) using GPS: involving relative rotation between the Turkish and Eurasian plates at $1.2^\circ \text{ Ma}^{-1}$ about $30.7^\circ \text{N } 32.6^\circ \text{E}$. This Euler vector predicts a rate of relative motion between these plates of $\sim 25 \text{ mm a}^{-1}$, which when extrapolated overestimates the observed amount of localised right-lateral slip; suggesting the existence of a component of distributed right-lateral simple shear in the surroundings to the NAFZ as well.

The predicted rate of left-lateral relative motion on the TR-AF plate boundary is estimated as $\sim 8 \text{ mm a}^{-1}$. However, the rate of localised left-lateral slip on the onshore part of this boundary is estimated as only $\sim 2 \text{ mm a}^{-1}$, on the Yakapınar-Göksun Fault: the difference being taken up by distributed deformation within the northern "promontory" of the African plate, which appears to involve a combination of anticlockwise rotation and distributed left-lateral simple shear. It is proposed that this boundary first developed at the same time as the NAFZ, but its original geometry involving left-lateral slip on the Karataş-Osmaniye Fault has since become locked by the presence of relatively strong ophiolitic crust within this fault zone.

The kinematic consistency of this model requires one to relax the assumption that brittle upper crust and mantle lithosphere are moving in step, consistent with the assumed presence of a weak layer of lower crust in between. The development of the NAFZ during the Messinian can thus be explained as a consequence of a combination of forces resulting from (a) shear tractions applied to the brittle upper crust of Turkey as a result of relative westward motion of mantle lithosphere, caused by the pre-existing relative motions between Africa and Arabia during the earlier Miocene; and (b) the reduction in normal stress and increase in right-lateral shear stress that resulted from the dramatic water unloading during the Messinian desiccation of the Mediterranean Basin. Analysis indicates that this mechanism requires the effective viscosity of the lower crust of Turkey to be $\sim 5 \pm 3 \times 10^{19} \text{ Pa s}$, consistent with recent estimates in other localities. The well-documented near-total absence of internal deformation within the Turkish plate thus does not result from high strength: it results from the

geometry of its boundaries which allow them to slip without any need for internal deformation. The main imperfection in this pattern of boundaries results from the high-strength “patch” on the TR-AF boundary in southern Turkey. The seismicity in this locality appears correlated with major earthquakes on the NAFZ, suggesting the possibility that this boundary behaves as a “geometrical lock” whose slip, in moderate-sized earthquakes, can permit much larger amounts of slip in much larger earthquakes on the NAFZ. Future detailed monitoring of this region may thus provide the basis for a system of advance warning of future destructive earthquakes on the NAFZ.

References

- AKTAR, M., ERGIN, M., ÖZALAYBEY, S., TAPIRDAMAZ, C., YÖRÜK, A. & BIÇMEN, F. 2000. A lower-crustal event in the northeastern Mediterranean: the 1998 Adana earthquake ($M_w=6.2$) and its aftershocks. *Geophysical Research Letters* **27**, 2361–2364.
- AMBRASEYS, N.N. & BARAZANGI, M. 1989. The 1759 earthquake in the Bekaa Valley: Implications for earthquake hazard assessment in the eastern Mediterranean region. *Journal of Geophysical Research* **94**, 4007–4013.
- AKSU, A.E., CALON, T.J., PIPER, D.J.W., TURGUT, S. & İZDAR, E. 1992a. Architecture of late orogenic Quaternary basins in northeastern Mediterranean Sea. *Tectonophysics* **210**, 191–213.
- AKSU, A.E., ULUÇ, A., PIPER, D.J.W., KONUK, Y.T. & TURGUT, S. 1992b. Quaternary sedimentary history of Adana, Cilicia and Iskenderun Basins: northeast Mediterranean Sea. *Marine Geology* **104**, 55–71.
- AMBRASEYS, N.N., 1988. Engineering seismology. *Earthquake Engineering and Structural Dynamics* **17**, 1–105.
- AMBRASEYS, N.N. & BARAZANGI, M. 1989. The 1759 earthquake in the Bekaa Valley: Implications for earthquake hazard assessment in the eastern Mediterranean region. *Journal of Geophysical Research* **94**, 4007–4013.
- ARGER, J., MITHCHEL, J. & WESTAWAY, R. 2000. Neogene and Quaternary volcanism of south-eastern Turkey. In: BOZKURT, E., WINCHESTER, J.A. & PIPER, J.D.A. (eds), *Tectonics and Magmatism of Turkey and the Surrounding Area*. Geological Society, London, Special Publications **173**, 459–487.
- ARMIJO, R., MEYER, B., HUBERT, A. & BARKA, A.A. 1999. Westward propagation of the North Anatolian Fault into the northern Aegean: Timing and kinematics. *Geology* **27**, 267–270.
- ARMIJO, R., MEYER, B., HUBERT, A. & BARKA, A.A. 2000. Reply to comment by Yaltrak, C., Sakiç, M., Oktay, F.Y., on “Westward propagation of the North Anatolian fault into the northern Aegean: Timing and kinematics”. *Geology* **28**, 188–189.
- ARPAT, E. & ŞAROĞLU, F. 1972. The East Anatolian Fault System: thoughts on its development. *General Directorate of Mineral Research and Exploration (MTA) Bulletin* **78**, 33–39.
- ATAN, O. 1969. *Eğribucak-Karacören (Hassa)-Ceylanlı-Dazevleri (Kırıkhan) Arasındaki Amanos Dağlarının Jeolojisi [Geology of Amanos Mountains in the Area between Eğribucak-Karacören (Hassa) and Ceylanlı-Dazevleri (Kırıkhan)]*. General Directorate of Mineral Research and Exploration (MTA) Report No. **139** [in Turkish, unpublished].
- BARKA, A.A. & KADINSKY-CADE, C. 1988. Strike-slip fault geometry in Turkey and its influence on earthquake activity. *Tectonics* **7**, 663–684.
- BEN-MENAHEM, Z. 1981. Variation of slip and creep along the Levant Rift over the past 4500 years. *Tectonophysics* **80**, 183–197.
- BESANÇON, J. & SANLAVILLE, P. 1993. La vallée de l’Oronte entre Rastane et Aacharné. In: SANLAVILLE, P., BESANÇON, J., COPELAND, L. & MUHESEN, S. (eds), *Le Paléolithique de la vallée moyenne de l’Oronte (Syrie): Peuplement et environnement*. British Archaeological Review, International Series **587**, 13–39.
- BOURCART, J. 1940. Recherches stratigraphiques sur le Pliocène et le Quaternaire du Levant. *Bulletin de la Société Géologique de France* **10**, 207–230.
- BREW, G., LUPA, J., BARAZANGI, M., SSWAF, T., AL-IMAM, A. & ZAZA, T. 2001. Structure and tectonic development of the Ghab Basin and the Dead Sea Fault System, Syria. *Journal of the Geological Society of London* **158**, 665–674.
- BRIDGLAND, D.R., PHILIP, G., WESTAWAY, R. & WHITE, M. 2003. A long Quaternary terrace sequence in the valley of the River Orontes, near Homs, Syria. *Current Science*, in press.
- BUTLER, R.W.H. & SPENCER, S. 1999. Landscape evolution and the preservation of tectonic landforms along the northern Yammouneh Fault, Lebanon. In: SMITH, B.J., WHALLEY W.B. & WARKE, P.A. (eds), *Uplift, Erosion, and Stability: Perspectives on Long-term Landscape Development*. Geological Society, London, Special Publications **162**, 143–156.

Acknowledgements

I would like to thank the many people who have collaborated with me in the field in the present study region, or have provided technical or logistical support or stimulating discussions, during this programme of research that began in Turkey in 1988 and in Syria in 2001. I particularly thank Jan Arger, Erdin Bozkurt, David Bridgland, Maryam Bshesh, Tuncer Demir, Francisco “Paco” Gomez, Mustapha Meghraoui, John Mitchell, Graham Philip, Saadettin Tonbul, and Sema Yurtmen.

- BUTLER, R.W.H., SPENCER, S. & GRIFFITHS, H.M. 1997. Transcurrent fault activity on the Dead Sea Transform in Lebanon and its implications for plate tectonics and seismic hazard. *Journal of the Geological Society of London* **153**, 757–760.
- BUTLER, R.W.H., GRIFFITHS, H.M. & SPENCER, S. 1998. The structural response to evolving plate kinematics during transpression; evolution of the Lebanese restraining bend of the Dead Sea Transform. In: HOLDSWORTH, R.E., STRACHAN, R.A. & DEWEY, J.F. (eds), *Continental Transpressional and Transtensional Tectonics*. Geological Society, London, Special Publications **135**, 81–106.
- ÇETİN, H. 2000. Paleoseismology of the Ecemiş Fault: mid results. In: *Workshop on Active Tectonics of Western Turkey, in Memoriam to Paul L. Hancock, Istanbul Technical University, June 2000, Abstract and Programme Volume*, 47–55.
- CHAIMOV, T.A., BARAZANGI, M., AL-SAAD, D., SSWAF, T. & GEBRAN, A. 1990. Crustal shortening in the Palmyride fold belt, Syria, and implications for movement along the Dead Sea Fault System. *Tectonics* **9**, 1369–1386.
- CHU DEZHI & GORDON, R.G. 1998. Current plate motions across the Red Sea. *Geophysical Journal International* **135**, 313–328.
- ÇOŞKUN, B. & ÇOŞKUN, B. 2000. The Dead Sea Fault and related subsurface structures, Gaziantep Basin, southeast Turkey. *Geological Magazine* **137**, 175–192.
- DEWEY, J.F., HEMPTON, M.R., KIDD, W.S.F., ŞAROĞLU, F. & ŞENGÖR, A.M.C. 1986. Shortening of continental lithosphere: the neotectonics of Eastern Anatolia - a young collision zone. In: COWARD, M.P. & RIES, A.C. (eds), *Collision Tectonics*. Geological Society, London, Special Publications **19**, 3–36.
- DOMAS, Y. 1994. The Late Cenozoic of the Al Ghab Rift, NW Syria. *Sbornik Geologických Ved, Antropozoikum* **21**, 57–73.
- DODONOV, A.E., DEVIATKIN, E.V., RANOV, V.A., KHATIB, K. & NSEIR, H. 1993. The Latamne Formation in the Orontes river valley. In: SANLAVILLE, P., BESANÇON, J., COPELAND, L. & MUHESEN, S. (eds), *Le Paléolithique de la vallée moyenne de l'Oronte (Syrie): Peuplement et environnement*. British Archaeological Review, International Series **587**, 189–194.
- DUBERTRET, L. & VAUTRIN, H. 1938. Sur l'existence du Pontien lacustre en Syrie et sur sa signification tectonique. *Comptes Rendus Hebdomadaires des Séances de l'Académie des Sciences de Paris* **206**, 69–71.
- EYAL, M., EYAL, Y., BARTOV, Y. & STEINITZ, G. 1981. The tectonic development of the western margins of the Gulf of Elat (Aqaba) rift. *Tectonophysics* **80**, 39–66.
- FREUND, R., GARFUNKEL, Z., ZAK, I., GOLDBERG, M., WEISSBROD, T. & DERIN, B. 1970. The shear along the Dead Sea Rift. *Philosophical Transactions of the Royal Society of London, Series A* **267**, 107–130.
- GARFUNKEL, Z. 1981. Internal structure of the Dead Sea leaky transform (rift) in relation to plate kinematics. *Tectonophysics* **80**, 81–108.
- GINAT, H., ENZEL, Y. & AVNİ, Y. 1998. Translocated Plio-Pleistocene drainage systems along the Arava Fault of the Dead Sea Transform. *Tectonophysics* **284**, 151–160.
- GIRDLER, R.W. 1990. The Dead Sea transform fault system. *Tectonophysics* **180**, 1–13.
- GOMEZ, F., MEGHRAOUI, M., DARKAL, A.N., SBEINATI, R., DARAWCHEH, R., TABEL, C., KHAWLIE, M., CHARABE, M., KHAIR, K. & BARAZANGI, M. 2001. Coseismic displacements along the Serghaya Fault: an active branch of the Dead Sea Fault System in Syria and Lebanon. *Journal of the Geological Society of London* **158**, 405–408.
- HANCOCK, P.L. & ATIYA, M.S. 1979. Tectonic significance of meso-fracture systems associated with the Lebanese segment of the Dead Sea transform fault. *Journal of Structural Geology* **1**, 143–153.
- HEIMANN, A. 2001. Stages in the development of the northern Dead Sea Transform. *Fourth International Turkish Geology Symposium, September 2001, Abstracts, Çukurova University, Adana, Turkey*, p. 181.
- Hsü, K.J. & GIAVANOLI, F. 1979. Messinian event in the Black Sea. *Palaeogeography, Palaeoclimatology, Palaeoecology* **29**, 75–93.
- İLKIŞIK, O.M. 1995. Regional heat flow in western Anatolia using silica temperature estimates from thermal springs. *Tectonophysics* **244**, 175–184.
- İLKIŞIK, O. M., GÜRER, A., TOKGÖZ, T. & KAYA, C. 1997. Geoelectromagnetic and geothermic investigations in the Ihlara Valley geothermal field. *Journal of Volcanology and Geothermal Research* **78**, 297–308.
- JACKSON, J.A. & MCKENZIE, D.P. 1988. The relationship between plate motions and seismic moment tensors, and the rates of active deformation in the Mediterranean and Middle East. *Geophysical Journal* **93**, 45–73.
- KAHLE, H.-G., COCARD, M., PETER, Y., GEIGER, A., REILINGER, R.E., BARKA, A.A. & VEIS, G. 2000. GPS-derived strain rate field within the boundary zones of the Eurasian African, and Arabian plates. *Journal of Geophysical Research* **105**, 23353–23370.
- KARİG, D.E. & KOZLU, H. 1990. Late Palaeogene–Neogene evolution of the triple junction near Maraş, south-central Turkey. *Journal of the Geological Society, London* **147**, 1023–1034.
- KAUFMAN, A., YECHIELI, Y. & GARDOSH, M. 1992. Reevaluation of the lake-sediment chronology in the Dead Sea basin, Israel, based on new ²³⁰Th/U dates. *Quaternary Research* **38**, 292–304.
- KEMPLER, D. & GARFUNKEL, Z. 1994. Structures and kinematics in the northeastern Mediterranean: a study of an irregular plate boundary. *Tectonophysics* **234**, 19–32.
- KHAIR, K., TSOKAS, G.N. & SAWAF, T. 1997. Crustal structure of the northern Levant region. Multiple source Werner deconvolution estimates for Bouguer gravity anomalies. *Geophysical Journal International* **126**, 605–616.
- KLINGER, Y., AVOUAC, J.P., ABOU KARAKI, N., DORBATH, L., BOURLES, D. & REYSS, J.L. 2000. Slip rate on the Dead Sea transform fault in northern Arava Valley (Jordan). *Geophysical Journal International* **142**, 755–768.

- KOZLOV, V., ARTEMOV, A. & KALIS, A. 1963. *Geological Map of the Trablus (I-36-XVIII) and Homs (I-37-XIII) Quadrangles, 1:200,000 Scale, and Accompanying Explanatory Guide*. Vsesoj. Exportno-Import Objed. Technoexport, Moscow, and Ministry of Industry, Syrian Arab Republic, Damascus.
- LE PICHON, X., LYBÉRIS, N. & ALVAREZ, F. 1984. Subsidence history of the North Aegean Trough. In: DIXON, J.E. & ROBERTSON, A.H.F. (eds), *The Geological Evolution of the Eastern Mediterranean*. Geological Society, London, Special Publications 17, 727–741.
- LOVELOCK, P.E.R. 1984. A review of the tectonics of the northern Middle East region. *Geological Magazine* 121, 577–587.
- MATAR, A. & MASCLE, G. 1993. Cinématique de la Faille du Levant au nord de la Syrie: analyse microtectonique du Fosse d'Alghab. *Geodinamica Acta* 6, 153–160.
- MCCCLUSKY, S.C., BALASSANIAN, S., BARKA, A.A., ERGINTAV, S., GEORGIEV, I., GÜRKAN, O., HAMBURGER, M., HURST, K., KAHLE, H., KASTENS, K., KEKELIDSE, G., KING, R., KOTZEV, V., LENK, O., MAHMOUD, S., MISHIN, A., NADARIA, M., OUZOUNIS, A., PARADISSIS, D., PETER, Y., PRILEPIN, M., REILINGER, R.E., ŞANLI, I., SEEGER, H., TEABLE, A., TOKSÖZ, N. & VEIS, G. 2000. Global Positioning System constraints on plate kinematics and dynamics in the eastern Mediterranean and Caucasus. *Journal of Geophysical Research* 105, 5695–5719.
- McKENZIE, D.P. 1976. The East Anatolian Fault: A major structure in eastern Turkey. *Earth and Planetary Science Letters* 29, 189–193.
- MEGHRAOUI, M. 2002. Large earthquake sequences along main continental faults: paleoseismic and historical constraints of the faulting behaviour. In: *First International Symposium of the Faculty of Mines, İstanbul Technical University, on Earth Sciences and Engineering, Abstracts*, p. 57.
- MICHARD, A., WHITECHURCH, H., RICOU, L.E., MONTIGNY, R. & YAZGAN, E. 1984. Tauric subduction (Malatya-Elazığ provinces) and its bearing on tectonics of the Tethyan realm in Turkey. In: DIXON, J.E. & ROBERTSON, A.H.F. (eds), *The Geological Evolution of the eastern Mediterranean*. Geological Society, London, Special Publications 17, 362–373.
- MITCHELL, J. & WESTAWAY, R. 1999. Chronology of Neogene and Quaternary uplift and magmatism in the Caucasus: Constraints from K-Ar dating of volcanism in Armenia. *Tectonophysics* 304, 157–186.
- MOUSTAFA, A.R. 1993. Structural characteristics and tectonic evolution of the east-margin blocks of the Suez rift. *Tectonophysics* 223, 381–399.
- MOUTY, M., DELALOYE, M., FONTIGNIE, D., PIŞKIN, O. & WAGNER, J.J. 1992. The volcanic activity in Syria and Lebanon between Jurassic and Actual. *Schweizerische Mineralogische und Petrographische Mitteilungen* 72, 91–105.
- MUEHLBERGER, W.B. & GORDON, M.B. 1987. Observations on the complexity of the East Anatolian Fault, Turkey. *Journal of Structural Geology* 9, 899–903.
- PERİNÇEK, D. & ÇEMEN, İ. 1990. The structural relationship between the East Anatolian and Dead Sea fault zones in southeastern Turkey. *Tectonophysics* 172, 331–340.
- PERİNÇEK, D. & KOZLU, H. 1983. Stratigraphy and structural relations of the units of the Afşin-Elbistan-Doğuşehir region (eastern Taurus). In: TEKELİ, O. & GÖNCÜOĞLU, M.C. (eds), *Geology of the Taurus Belt*. Proceedings of International Symposium on the Geology of the Taurus Belt, 1983. General Directorate of Mineral Research and Exploration (MTA) Publication, 181–198.
- PFISTER, M., RYBACH, L. & ŞİMŞEK, Ş. 1998. Geothermal reconnaissance of the Marmara Sea region (NW Turkey); surface heat flow density in an area of active continental extension. *Tectonophysics* 291, 77–89.
- PONIKAROV, V.P., KAZMIN, V.G., MIKHAILOV, I.A., RAZVALIYEV, A.V., KRASHENINNIKOV, V.A., KOZLOV, V.V., SOULIDI-KONDRATIYEV, E.D. & FARADZHEV, V.A. 1966. *The Geological Map of Syria, 1:1,000,000: Scale, and Accompanying Explanatory Guide*. Vsesoj. Exportno-Import Objed. Technoexport, Moscow, and Ministry of Industry, Syrian Arab Republic, Damascus.
- PONIKAROV, V.P., KAZMIN, V.G., MIKHAILOV, I.A., RAZVALIYEV, A.V., KRASHENINNIKOV, V.A., KOZLOV, V.V., SOULIDI-KONDRATIYEV, E.D., MIKHAILOV, K.Y., KULAKOV, V.A., FARADZHEV, V.A. & MIRZAYEV, K.M. 1967. *The Geology of Syria: Explanatory Notes on the Geological Map of Syria, Scale 1:500,000. Part I: Stratigraphy, Igneous Rocks, and Tectonics*. Vsesoj. Exportno-Import Objed. Technoexport, Moscow, and Ministry of Industry, Syrian Arab Republic, Damascus.
- QUENNEL, A.M. 1984. The Western Arabia rift system. In: DIXON, J.E. & ROBERTSON, A.H.F. (eds), *The Geological Evolution of the Eastern Mediterranean*. Geological Society, London, Special Publications 17, 375–402.
- RYAN, W.B.F. & CITA, M.B. 1978. The nature and distribution of Messinian erosional surfaces – Indicators of a several-kilometer deep Mediterranean in the Miocene. *Marine Geology* 27, 193–230.
- REILINGER, R.E., MCCCLUSKY, S.C., ORAL, M.B., KING, W. & TOKSÖZ, M.N. 1997. Global Positioning System measurements of present-day crustal movements in the Arabian-Africa-Eurasia plate collision zone. *Journal of Geophysical Research* 102, 9983–9999.
- ŞAROĞLU, F., EMRE, Ö. & KUŞÇU, İ. 1992. The East Anatolian Fault Zone of Turkey. *Annales Tectonicae* 6, 99–125.
- ŞENGÖR, A.M.C., GÖRÜR, N. & ŞAROĞLU, F. 1985. Strike-slip faulting and basin formation in zones of tectonic escape: Turkey as a case study. In: BIDDLE, K.T. & CHRISTIE-BLICK, N. (eds), *Strike-slip Faulting and Basin Formation*. Society of Economic Mineralogists and Petrologists Special Publication 37, 227–264.
- SHATSKY, V.N., KAZMIN, V.G. & KULAKOV, V.V. 1963. *Geological Map of the Al-Latheqieh (I-36-XXIV) and Hama (I-37-XIX) Quadrangles, 1:200,000 Scale, and Accompanying Explanatory Guide*. Vsesoj. Exportno-Import Objed. Technoexport, Moscow, and Ministry of Industry, Syrian Arab Republic, Damascus.

- STEINITZ, G., BARTOV, Y., EYAL, M. & EYAL, Y. 1981. K-Ar age determination of Tertiary magmatism along the western margin of the Gulf of Elat. *Geological Survey of Israel Current Research for 1980*, 27–29.
- STRAUB, C., KAHLE, H.-G. & SCHINDLER, C. 1997. GPS and geologic estimates of the tectonic activity in the Marmara Sea region, NW Anatolia. *Journal of Geophysical Research* **102**, 27587–27601.
- TEN BRINK, U.S., RYBAKOV M., AL-ZOUBI, A.S., HASSOUNEH, M., FRIESLANDER, U., BATAYNEH, A.T., GOLDSCHMIDT, V., DAUD, M.N., ROTSTEIN, Y. & HALL, J.K. 1999. Anatomy of the Dead Sea transform: does it reflect continuous changes in plate motion? *Geology* **27**, 887–890.
- TERLEMEZ., H.C.İ., ŞENTÜRK, K., ATEŞ, Ş. & ORAL, A. 1997. *Geological Map of the Gaziantep-K24 Quadrangle, 1:100,000 Scale, and Accompanying 18 page Explanatory Booklet*. General Directorate of Mineral Research and Exploration (MTA) Publication.
- TOLUN, N. & ERENTÖZ, C. 1962. *Hatay Sheet of the Geological Map of Turkey, 1:500,000 Scale*. General Directorate of Mineral Research and Exploration (MTA) Publication.
- TOLUN, N. & PAMIR, H.N. 1975. *Explanatory Booklet Accompanying the Hatay Sheet of the Geological Map of Turkey, 1:500,000 Scale*. General Directorate of Mineral Research and Exploration (MTA) Publication.
- TÜYSÜZ, O., BARKA, A.A. & YİĞİTBAŞ, E. 1998. Geology of the Saros graben and its implications for the evolution of the North Anatolian fault in the Ganos-Saros region, northwestern Turkey. *Tectonophysics* **293**, 105–126.
- VAN LIERE, W.J. 1961. Observations on the Quaternary in Syria. *Berichten Rijksd. Ovdheidk. Bodemonderzoek* **11**, 7–69.
- DE VAUMAS, E. 1957. Plateaux, plaines et dépressions de la Syrie intérieure septentrionale: Étude morphologique. *Bulletin de la Société de Géographie d'Égypte* **30**, 97–236.
- VIDAL, N., ALVAREZ-MARRON, J. & KLAESCHEN, D. 2000. Internal configuration of the Levantine Basin from seismic reflection data (eastern Mediterranean). *Earth and Planetary Science Letters* **180**, 77–89.
- WALLEY, C.D. 1988. A braided strike-slip model for the northern continuation of the Dead Sea Fault and its implications for Levantine tectonics. *Tectonophysics* **145**, 63–72.
- WALLEY, C.D. 1998. Some outstanding issues in the geology of Lebanon and their importance in the tectonic evolution of the Levantine region. *Tectonophysics* **298**, 37–62.
- WESTAWAY, R. 1990. Present-day kinematics of the plate boundary zone between Africa and Europe, from the Azores to the Aegean. *Earth and Planetary Science Letters* **96**, 393–406.
- WESTAWAY, R. 1993. Forces associated with mantle plumes. *Earth and Planetary Science Letters* **119**, 331–348.
- WESTAWAY, R. 1994a. Present-day kinematics of the Middle East and eastern Mediterranean. *Journal of Geophysical Research* **99**, 12071–12090.
- WESTAWAY, R. 1994b. Evidence for dynamic coupling of surface processes with isostatic compensation in the lower crust during active extension of western Turkey. *Journal of Geophysical Research* **99**, 20203–20223.
- WESTAWAY, R. 1994c. Reevaluation of extension in the Pearl River Mouth basin, South China Sea: Implications for continental lithosphere deformation mechanisms. *Journal of Structural Geology* **16**, 823–838.
- WESTAWAY, R. 1995a. Deformation around stepovers in strike-slip fault zones. *Journal of Structural Geology* **17**, 831–847.
- WESTAWAY, R. 1995b. Crustal volume balance during the India-Eurasia collision and altitude of the Tibetan plateau: a working hypothesis. *Journal of Geophysical Research* **100**, 15173–15194.
- WESTAWAY, R. 1996. Quaternary elevation change in the Gulf of Corinth of central Greece. *Philosophical Transactions of the Royal Society of London, Series A* **354**, 1125–1164.
- WESTAWAY, R. 1998. Dependence of active normal fault dips on lower-crustal flow regimes. *Journal of the Geological Society, London* **155**, 233–253.
- WESTAWAY, R. 1999a. The mechanical feasibility of low-angle normal faulting. *Tectonophysics* **308**, 407–443 (Correction: *Tectonophysics* **341**, 237–238, 2001).
- WESTAWAY, R. 1999b. Comment on "A new intracontinental transcurrent structure: The Central Anatolian Fault Zone, Turkey, by A. Koçyiğit and A. Beyhan". *Tectonophysics* **314**, 469–479.
- WESTAWAY, R. 2001. Flow in the lower continental crust as a mechanism for the Quaternary uplift of the Rhenish Massif, north-west Europe. In: MADDY, D., MACKLIN, M.G. & WOODWARD, J.C. (eds), *River Basin Sediment Systems: Archives of Environmental Change*. Balkema, Abingdon, England, 87–167.
- WESTAWAY, R. 2002a. Discussion of "New sedimentological and structural data from the Ecemiş Fault Zone, southern Turkey: implications for its timing and offset and the Cenozoic tectonic escape of Anatolia" by Jaffey, N. & Robertson, A.H.F. *Journal of the Geological Society, London* **159**, 111–113.
- WESTAWAY, R. 2002b. The Quaternary evolution of the Gulf of Corinth, central Greece: coupling between surface processes and flow in the lower continental crust. *Tectonophysics* **348**, 269–318.
- WESTAWAY, R. 2002c. Geomorphological consequences of weak lower continental crust, and its significance for studies of uplift, landscape evolution, and the interpretation of river terrace sequences. *Netherlands Journal of Geosciences* **81**, 283–304.
- WESTAWAY, R. 2002d. Long-term river terrace sequences: Evidence for global increases in surface uplift rates in the Late Pliocene and early Middle Pleistocene caused by flow in the lower continental crust induced by surface processes. *Netherlands Journal of Geosciences* **81**, 305–328.
- WESTAWAY, R. 2002e. Seasonal seismicity of northern California before the great 1906 earthquake. *Pure and Applied Geophysics* **159**, 7–62.

- WESTAWAY, R. & ARGER, J. 1996. The Gölbaşı basin, southeastern Turkey: A complex discontinuity in a major strike-slip fault zone. *Journal of the Geological Society, London* **153**, 729–743.
- WESTAWAY, R. & ARGER, J. 2001. Kinematics of the Malatya-Ovacık Fault Zone. *Geodinamica Acta* **14**, 103–131.
- WESTAWAY, R., MADDY, D. & BRIDGLAND, D.R. 2002. Flow in the lower continental crust as a mechanism for the Quaternary uplift of southeast England: constraints from the Thames terrace record. *Quaternary Science Reviews* **21**, 559–603.
- WESTAWAY, R., PRINGLE, M., YURTMEN, S., DEMİR, T., BRIDGLAND, D., ROWBOTHAM, G. & MADDY, D. 2003. Pliocene and Quaternary surface uplift of western Turkey revealed by long-term river terrace sequences. *Current Science*, in press.
- WILLIS, B. 1928. Earthquakes in the Holy Land. *Bulletin of the Seismological Society of America* **18**, 73–103.
- YALTIRAK, C., SŞAKINÇ M. & OKTAY, F.Y. 2000. Comment on “Westward propagation of the North Anatolian fault into the northern Aegean: Timing and kinematics” by Armijo, R., Meyer, B., Hubert, A. & Barka, A.A.. *Geology* **28**, 187–188.
- YAZGAN, E. 1983. Geodynamic evolution of the Eastern Taurus region. In: TEKELİ, O. & GÖNCÜOĞLU, M.C. (eds), *Geology of the Taurus Belt*. Proceedings of International Symposium on the Geology of the Taurus Belt, 1983. General Directorate of Mineral Research and Exploration (MTA) Publication, 199–208.
- YURTMEN, S. & WESTAWAY, R. 2001a. *Intraplate Alkaline Volcanism to the North of İskenderun Gulf*. Field Excursion Guide Book, Fourth International Turkish Geology Symposium. Çukurova University, Adana, Turkey.
- YURTMEN, S. & WESTAWAY, R. 2001b. Neogene to Quaternary volcanism and strike-slip faulting in the Gaziantep Plateau, southeastern Turkey. *Fourth International Turkish Geology Symposium, September 2001, Çukurova University, Adana, Turkey, Abstracts*, p. 184.
- YURTMEN, S., GUILLOU, H., WESTAWAY, R., ROWBOTHAM, G. & TATAR, O. 2002. Rate of strike-slip motion on the Amanos Fault (Karasu Valley, southern Turkey) constrained by K-Ar dating and geochemical analysis of Quaternary basalts. *Tectonophysics* **344**, 207–246.
- YURTMEN, S., ROWBOTHAM, G., İŞLER, F. & FLOYD, P. 2000. Petrogenesis of Quaternary alkali volcanics, Ceyhan - Turkey. In: BOZKURT, E., WINCHESTER, J.A. & PIPER, J.D.A. (eds), *Tectonics and Magmatism of Turkey and the Surrounding Area*. Geological Society, London, Special Publications **173**, 489–512.
- ZHANG, H. 1998. *Late Pleistocene and Holocene Slip Rate of the Northern Wadi Araba Fault, Dead Sea Transform, Jordan*. MSc Thesis, University of Missouri Kansas City, Kansas City, Missouri, USA [unpublished].

Received 16 May 2002; revised typescript accepted 05 January 2003